

Likelihood-based Inference for Partially Observed Epidemics on Dynamic Networks

Fan Bu¹, Allison E. Aiello², Jason Xu^{*§1}, and Alexander Volfovsky^{*1}

¹Department of Statistical Science, Duke University

²Gillings School of Global Public Health, University of North Carolina at Chapel Hill[†]

Abstract

We propose a generative model and an inference scheme for epidemic processes on dynamic, adaptive contact networks. Network evolution is formulated as a link-Markovian process, which is then coupled to an individual-level stochastic SIR model, in order to describe the interplay between epidemic dynamics on a network and network link changes. A Markov chain Monte Carlo framework is developed for likelihood-based inference from partial epidemic observations, with a novel data augmentation algorithm specifically designed to deal with missing individual recovery times under the dynamic network setting. Through a series of simulation experiments, we demonstrate the validity and flexibility of the model as well as the efficacy and efficiency of the data augmentation inference scheme. The model is also applied to a recent real-world dataset on influenza-like-illness transmission with high-resolution social contact tracking records.

Keywords: stochastic susceptible-infectious-recovered (SIR) model, continuous-time Markov processes, Bayesian data augmentation, conditional simulation, mobile healthcare, network inference.

^{*}Joint last authors. [§]Corresponding author: jason.q.xu@duke.edu

[†]The eXFLU data were supported by U01 CK000185, AV and AA were partially supported by R01 EB025021, AV and FB were partially supported by W911NF1810233, JX was partially supported by DMS 1606177.

1 Introduction

The vast majority of epidemiological models, such as the well-known susceptible-infected-recovered (SIR) model, rely on compartmentalizing individuals according to their disease status, meaning that individual level information is lost (Kermack and McKendrick, 1927). Classical compartmental models adopt the “random mixing” assumption under which an infectious individual can spread the disease homogeneously to any susceptible individual (Kermack and McKendrick, 1927; Bailey et al., 1975; Anderson and May, 1992). In the last two decades, an alternative assumption—that the disease is transmitted through links in a contact network—has gradually gained popularity. As a result, there has been an increase in the relevance and importance of networks in transmittable disease research.

Networks can flexibly and informatively represent human interactions, contact patterns, and social structures, which can fundamentally impact the behavior of epidemic processes (Wallinga et al., 1999; Edmunds et al., 1997, 2006; Mossong et al., 2008; Melegaro et al., 2011). Also, there is evidence that the population network structure can be influenced by infection events as well (Bell et al., 2006; Funk et al., 2010; Eames et al., 2010; Van Kerckhove et al., 2013). Numerous recent epidemiological methods consider both disease transmission and the contact network as dynamic processes (Bansal et al., 2010; Pastor-Satorras et al., 2015; Masuda and Holme, 2013; Enright and Kao, 2018; Masuda and Holme, 2017), and even as *coupled* processes: disease spread is impacted by the evolving network structure, which also *adapts* to contagion progression in that individuals with different health statuses adopt different social behaviors (Kiss et al., 2012; Ogura and Preciado, 2017; Van Segbroeck et al., 2010; Tunc et al., 2013; Group, 2006).

In this paper, we propose a stochastic generative model that jointly describes SIR-type epidemic processes on temporal networks *and* dynamics of adaptive networks, and then develop a likelihood-based Bayesian inference scheme that accommodates missingness in individual epidemic recovery times. We choose stochastic models over deterministic models widely used in existing literature to account for the randomness in small-scale epidemic outbreaks and allow for measures of uncertainty in estimation (Britton, 2010). The model formulation is also motivated by the increasing need for inference based on real-world epi-

demiological data that contain time-resolved social interactions data. Almost all previous methods for adaptive network epidemic processes focus on theoretical derivation or numerical simulation due to the long-standing difficulty in dynamically tracking social contacts. However, thanks to technological advancements in mobile devices, several recent observational studies have collected high-resolution data on social contacts (Vanhems et al., 2013; Barrat et al., 2014; Voirin et al., 2015; Kiti et al., 2016; Aiello et al., 2016; Ozella et al., 2018), which enables inference on the interplay between epidemic and network processes.

Moreover, real-world epidemiological data almost always contain some missingness, particularly in the exact times of individual disease episodes. This is a major challenge for inference, even without the additional complexity of network dynamics (Ho et al., 2018). To address this challenge, we design an inference scheme that includes a novel data augmentation algorithm that leverages both the network dynamics and the generative process implied by the model. This algorithm is, in principle, similar to existing agent-based data augmentation methods for fitting stochastic epidemic models that propose individual disease episodes compatible with the observations (Cauchemez et al., 2006; Hoti et al., 2009; Fintzi et al., 2017). It also bears some resemblance to simulation-based methods (Andrieu et al., 2010; Pooley et al., 2015) that use the underlying model to propose epidemic paths (yet at the population-level) as the foundation for inference. However, these methods are inadequate in coping with the intricate constraints imposed by time-varying social contacts, or utilizing network information to reduce the difficulty in evaluating the exact likelihood function. Moreover, these methods are computationally expensive, especially those based on simulations. In comparison, the data augmentation method introduced in this work is more effective and efficient.

This paper is organized as follows: Section 2 provides some background knowledge on epidemic models (the stochastic SIR model in particular), basic network concepts, and dynamic and adaptive network processes. Section 3 formulates the generative model and derives maximum likelihood estimators as well as Bayesian posterior distributions based on the complete data likelihood. Section 4 describes a Bayesian inference scheme that deals with incomplete observations on individual recovery times. Section 5 and 6 present experiment results on simulated datasets and a real-world dataset. Finally Section 7 gives further discussions.

2 Background

2.1 Compartmental Epidemiological Models

The vast majority of epidemiological models are based on compartmentalizing individuals into non-overlapping subsets according to their disease statuses. In classical models, the sizes of those subsets are described by differential equations (Hethcote, 2000). One famous and widely used model is the susceptible-infected-recovered (SIR) model, which assumes three disease statuses—susceptible (S), infected (or infectious, I), and recovered (or removed, R). On a closed population of N individuals (with N sufficiently large), the deterministic dynamics of the SIR model can be expressed as

$$\frac{dS(t)}{dt} = -\beta S(t)I(t), \quad \frac{dI(t)}{dt} = \beta S(t)I(t) - \gamma I(t), \quad (1)$$

where $S(t)$ and $I(t)$ refer to the number of susceptible and infected individuals at time t , respectively, and the number of recovered individuals satisfies $R(t) = N - [S(t) + I(t)]$. Here β is the rate of disease transmission per contact between an S individual and an I individual, and γ is the rate of recovery for an I individual.

By setting the growth rate of infection to be proportional to $S(t)I(t)$, the model in (1) implicitly assumes that any two members can interact with each other. This assumption is easily violated in reality, where an individual only maintains contact with a limited number of others. Moreover, the differential equations can only account for the average, expected behavior of the process, but the transmission of an infectious disease exhibits randomness and uncertainty by nature.

To account for the underlying network structure of a population as well as the random nature of an epidemic process, we adopt an *individual-level, stochastic* variation of the SIR model (similar to that used in Auranen et al. (2000)). An individual of status S (susceptible) at time t (> 0) changes disease status to I (infected/infectious) at time $t + h$ (h is an infinitesimal quantity) with a probability that is dependent on both the infection rate β and his/her contacts at time t . An infected individual at time t becomes a member of the R (recovered) sub-population at time $t + h$ with a probability determined by the recovery rate γ . Specifically, for any susceptible individual p_1 and infected individual p_2 in the population

at t , conditioned on the current overall state of the process, \mathcal{Z}_t , then

$$Pr(p_1 \text{ gets infected by } p_2 \text{ at } t + h | \mathcal{Z}_t) = \beta h + o(h) \quad (2)$$

if p_1 and p_2 are in contact at t , and

$$Pr(p_2 \text{ recovers at } t + h | \mathcal{Z}_t) = \gamma h + o(h). \quad (3)$$

2.2 Basic Network Concepts

A network, or a graph, is a two-component set, $\mathcal{G} = \{\mathcal{V}, \mathcal{E}\}$, where \mathcal{V} is the set of N nodes and \mathcal{E} is the set of links. A network can be represented by its “adjacency matrix”, \mathbf{A} , where $\mathbf{A}_{ij} = 1$ indicates there is a link from node i to j . Since most infectious diseases can be transmitted in both directions through a contact, we assume that the adjacency matrix is *symmetric*, $\mathbf{A}_{ij} = \mathbf{A}_{ji}$.

A special network structure is the fully connected network (or the complete graph), \mathcal{K}_N , and its adjacency matrix \mathbf{A} satisfies $\mathbf{A}_{ij} = 1$ for any $i \neq j$. This network structure corresponds to the widely adopted “random mixing” assumption in epidemiological models, which, as stated before, is unrealistic and restrictive. Therefore, in the rest of the paper, we consider *arbitrary* network structures on a population instead.

2.3 Temporal and Adaptive Networks

Interactions between individuals are dynamic in nature, and such dynamics is important when modeling epidemic processes (Masuda and Holme (2017); also as demonstrated later in Section 5.1). We consider a continuous-time link-Markovian model for temporal networks (Clementi et al., 2010; Ogura and Preciado, 2016). For two individuals i and j who are not in contact at time t , they form a link at time $t + h$ ($h \ll 1$) with probability αh , where α is the link activation rate. Similarly, if there is an edge between i and j at time t , then the edge is deleted at time $t + h$ with probability ωh , where ω is some link termination rate.

If, instead, individuals establish and dissolve their social links with rates that vary according to their disease statuses, then the evolution of the network is coupled to the epidemic process and thus becomes *adaptive*. This mechanism can be described by instantaneous rates

of single-link changes. For any two individuals i and j , their corresponding entry in the adjacency matrix can be thought of as a $\{0, 1\}$ -valued Markov process, $\mathbf{A}_{ij}(t), t > 0$. Suppose that at time t , i is of status A , j is of status B ,¹ then for an infinitesimal quantity h ,

$$Pr(\mathbf{A}_{ij}(t+h) = 1 | \mathbf{A}_{ij}(t) = 0) = \alpha_{AB}h + o(h); \quad (4)$$

$$Pr(\mathbf{A}_{ij}(t+h) = 1 | \mathbf{A}_{ij}(t) = 1) = \omega_{AB}h + o(h). \quad (5)$$

3 Adaptive Network Epidemic Processes and Inference with Complete Data

3.1 The Generative Model

In this subsection, we lay out a generative model for the joint evolution of an individualized SIR process on a networked population and the dynamics of the contact network. The key feature of the model is the *interplay* between epidemic progression and network adaptation: on one hand, transmission of infection depends on the existence of susceptible-infected links, which may change through time; on the other hand, network links temporally update in a manner that in turn depends on individual disease status.

We formulate this complex process as a continuous-time Markov process that comprises all the competing Poisson processes with exponentially-distributed wait times at the individual level, as described in (2)-(5). Throughout the process, the system is updated stochastically with one event (for one individual or a pair) at a time, and each event is of one of the four types:

- **Infection:** The disease is transmitted through a link between an S (susceptible) and an I (infected) individual (S - I link) with rate β ;
- **Recovery:** Each I individual recovers with rate γ independently;
- **Link activation:** A link is formed at rate α_{AB} between an individual of status A and another of status B who are not connected, where $A, B \in \{S, I, R\}$;

¹Here $A, B \in \{S, I, R\}$.

- **Link termination:** An existing link is removed at rate ω_{AB} between an individual of status A and another of status B , where $A, B \in \{S, I, R\}$.

This model formulation allows for joint inference of both disease spread and network evolution, and as illustrated in the next sub-section, inference is straightforward when all the events are fully observed. Furthermore, this formulation corresponds to a relatively simple generative process at the population level too. By the superposition property, conditioned on the current state of the process \mathcal{Z}_t at time $t (> 0)$, the very next event of the entire process is the *earliest* event that occurs among the four competing processes:

- **Infection:** An infection occurs with rate $\beta SI(t)$, where $SI(t)$ is the number of S - I links at time t ;
- **Recovery:** A recovery occurs with rate $\gamma I(t)$, where $I(t)$ is the number of infected individuals at time t ;
- **Link activation:** An A - B link is established with rate $\alpha_{AB} M_{AB}^d(t)$, where $M_{AB}^d(t)$ is the number of disconnected A - B pairs at time t ;
- **Link termination:** An A - B link is dissolved with rate $\omega_{AB} M_{AB}(t)$, where $M_{AB}(t)$ is the number of connected A - B pairs at time t .

This generative model is a generalization of two simpler models. If we set $\alpha_{AB} \equiv \alpha$ and $\omega_{AB} \equiv \omega$ for any status A and B , the coupled process is reduced to a *decoupled* process, where network evolution is *independent* of individual disease status. Moreover, if we fix $\alpha \equiv \omega \equiv 0$, the process is further reduced to an SIR process over a *static* network.

Here we assume that the population size N is fixed, and both the initial network structure \mathcal{G}_0 and the number of infection cases at onset, $I(0)$, are known. We summarize a list of important parameters and notation used for model formulation and inference in Table 1.

Table 1: Table of parameters and notation.

Parameter	Description
β	infection rate
γ	recovery rate
α	link activation rate for a currently disconnected pair
ω	link termination rate for a currently connected pair
α_{AB}	link activation rate for a currently disconnected A-B pair
ω_{AB}	link termination rate for a currently connected A-B pair
Notation	Description
N	total population size (assumed to remain fixed throughout the process)
T_{\max}	maximum observation time
\mathcal{Z}_t	state of the process at time t (including the epidemic status of every individual and the social network structure at time t)
\mathcal{G}_t	social network structure (a graph) at time t
$S(t), I(t)$	numbers of susceptible/infected individuals in the population at time t
$H(t)$	number of healthy (not infected) individuals in the population at time t
$I_k(t)$	number of infected individuals in person k 's neighborhood at time t
$SI(t)$	number of S-I links in the network at time t
$M(t)$	total number of edges in the network at time t
$M_{AB}(t)$	number of A-B links at time t
$M_{AB}^d(t)$	number of disconnected A-B pairs at time t
n_E, n_R	counts of infection events and recovery events in the process
n_N	count of network events in the process (each event is the activation or termination of a single link)
C, D	total counts of link activation/termination
C_{AB}, D_{AB}	counts of link activation/termination events for A-B pairs

3.2 Complete Data Likelihood and Parameter Estimation

Derivation of complete data likelihood Let i_k be the infection time for individual k ($k = 1, 2, \dots, n_E$), r'_k be the k' th observed recovery time ($k' = 1, 2, \dots, n_R$), and without

loss of generality, set $i_1 = 0$. Recall that the widely used “random mixing” assumption in classical epidemiological models is equivalent to assuming that the contact network is a complete graph, \mathcal{K}_N , and the complete data likelihood under this assumption is

$$\mathcal{L}(\beta, \gamma) = p(\text{epidemic events}|\beta, \gamma) = \gamma^{n_R} \prod_{k=2}^{n_E} [\beta I(i_k)] \exp \left(- \int_0^{T_{\max}} [\beta S(u)I(u) + \gamma I(u)] du \right).$$

Instead, assume that the network is an arbitrary *static* network \mathcal{G} . Then when writing down the complete data likelihood, we have to explicitly account for the number of infected contacts for each individual at the time of infection as well as the total number of S - I links in the system:

$$\mathcal{L}(\beta, \gamma|\mathcal{G}) = \gamma^{n_R} \prod_{k=2}^{n_E} [\beta I_k(i_k)] \exp \left(- \int_0^{T_{\max}} [\beta SI(u) + \gamma I(u)] du \right). \quad (6)$$

Here $I_k(t)$ denotes the number of infectious individuals that are connected to person k at time t , which remains fixed for a static network.

If the network is not static, but the *entire network process* $\{\mathcal{G}_t : 0 < t < T_{\max}\}$ is given (or all the network changes during the contagion process are fully observed), then the form of the data likelihood remains unchanged, *conditioned* on $\{\mathcal{G}_t\}$. Note that the dynamic nature of the network can be implicitly subsumed into the terms $I_k(i_k)$ ’s and $SI(u)$.

To incorporate network dynamics, we begin with the simpler *decoupled* process in which the network evolves *independently* of the epidemic process with edge activation rate α and deletion rate ω . Given the initial network \mathcal{G}_0 , the likelihood of the network process alone can be easily written down as

$$\begin{aligned} \mathcal{L}(\alpha, \omega|\mathcal{G}_0) &= p(\text{network events}|\alpha, \omega, \mathcal{G}_0) \\ &= \alpha^C \omega^D \prod_{\ell=1}^{n_N} \left[\left(\frac{N(N-1)}{2} - M(s_\ell) \right)^{1-D_\ell} M(s_\ell)^{D_\ell} \right] \\ &\quad \times \exp \left(-\alpha \frac{N(N-1)}{2} T_{\max} + (\alpha - \omega) \int_0^{T_{\max}} M(u) du \right). \end{aligned} \quad (7)$$

Here s_ℓ is the time of the ℓ th network event, and $D_\ell = 1$ if this event is a *link termination* and otherwise $D_\ell = 0$. Therefore, when the epidemic process and network process are decoupled, the complete data likelihood is simply a product of the terms in (6) and (7):

$$\mathcal{L}(\beta, \gamma, \alpha, \omega|\mathcal{G}_0) = p(\text{epidemic events}|\beta, \gamma, \mathcal{G}_t) p(\text{network events}|\alpha, \omega, \mathcal{G}_0)$$

$$\begin{aligned}
&= \beta^{n_E-1} \gamma^{n_R} \alpha^C \omega^D \prod_{k=2}^{n_E} [I_k(i_k)] \prod_{\ell=1}^{n_N} \left[\left(\frac{N(N-1)}{2} - M(s_\ell) \right)^{1-D_\ell} M(s_\ell)^{D_\ell} \right] \\
&\times \exp \left(- \int_0^{T_{\max}} [\beta SI(u) + \gamma I(u) + (\omega - \alpha)M(u)] du - \alpha \frac{N(N-1)}{2} T_{\max} \right).
\end{aligned} \tag{8}$$

Then we consider the coupled process with an *adaptive* network, where link activation and termination are dependent on individual disease status. Define $g(p, t)$ as the indicator function of infectiousness, i.e. $g(p, t) = 1$ if person p is infected at time t and $g(p, t) = 0$ otherwise. We further assume that the S and R populations behave identically in the network process:

$$\alpha_{R\cdot} \equiv \alpha_{S\cdot}, \text{ and } \omega_{R\cdot} \equiv \omega_{S\cdot}.$$

We shall refer to them as the “ H ” (healthy) population; let $H(t) = R(t) + S(t) = N - I(t)$ denote the number of healthy individuals at time t . Naturally the term “H-H link” represent an S-S link, an S-R link, or an R-R link, and the term “H-I link” represent either an S-I link or an R-I link.

Combine the epidemic events and network events and re-denote all events as $\{e_j = (t_j, p_{j1}, p_{j2})\}_{j=1}^n$, $n = n_E + n_R + n_N$. Here t_j is the event time (set $t_1 = 0$, the infection time of the first patient), with $t_1 < t_2 < \dots < t_n$. If e_j is a network event, p_{j1}, p_{j2} are the two individuals getting connected or disconnected, and if e_j is an epidemic event, let p_{j1} be the person getting infected or recovered and set $p_{j2} = 0$. Furthermore let event type indicators F_j, C_j, D_j take the value 1 only if e_j is an infection, a link activation, and a link deletion, respectively, and otherwise take the value 0.

The contribution of all network events to the complete data likelihood is in essence of the same form as (7), except that for every activation or termination event the link type has to be considered. Then the likelihood component of the adaptive network process is

$$\alpha_{SS}^{C_{HH}} \alpha_{SI}^{C_{HI}} \alpha_{II}^{C_{II}} \omega_{SS}^{D_{HH}} \omega_{SI}^{D_{HI}} \omega_{II}^{D_{II}} \prod_{j=2}^n \tilde{M}(t_j) \exp \left(- \int_0^{T_{\max}} [\tilde{\alpha}^T \mathbf{M}_{\max}(t) + (\tilde{\omega} - \tilde{\alpha})^T \mathbf{M}(t)] dt \right),$$

where

$$\begin{aligned}
\tilde{M}(t_j) &= [(\alpha_{SS} M_{HH}^d(t_j))^{C_j} (\omega_{SS} M_{HH}(t_j)^{D_j})]^{(1-g(p_{j1}, t_j))(1-g(p_{j2}, t_j))} \\
&\times [(\alpha_{SI} M_{HI}^d(t_j))^{C_j} (\omega_{SI} M_{HI}(t_j)^{D_j})]^{|g(p_{j1}, t_j) - g(p_{j2}, t_j)|}
\end{aligned} \tag{9}$$

$$\times [(\alpha_{II} M_{II}^d(t_j))^{C_j} (\omega_{II} M_{II}(t_j))^{D_j}]^{(p_{j1}, t_j)g(p_{j2}, t_j)}$$

$$\tilde{\alpha} = (\alpha_{SS}, \alpha_{SI}, \alpha_{II})^T, \quad (10)$$

$$\tilde{\omega} = (\omega_{SS}, \omega_{SI}, \omega_{II})^T, \quad (11)$$

$$\mathbf{M}_{\max}(t) = \left(\frac{H(t)(H(t)-1)}{2}, H(t)I(t), \frac{I(t)(I(t)-1)}{2} \right)^T, \quad (12)$$

$$\mathbf{M}(t) = (M_{HH}(t_j), M_{HI}(t), M_{II}(t))^T. \quad (13)$$

Therefore, given the initial network structure \mathcal{G}_0 and one infected case at time 0, the complete data likelihood can be expressed as

$$\begin{aligned} \mathcal{L}(\beta, \gamma, \tilde{\alpha}, \tilde{\omega} | \mathcal{G}_0) &= p(\text{epidemic events, network events} | \beta, \gamma, \tilde{\alpha}, \tilde{\omega}, \mathcal{G}_0) \\ &= \gamma^{n_R} \beta^{n_E-1} \alpha_{SS}^{C_{HH}} \alpha_{SI}^{C_{HI}} \alpha_{II}^{C_{II}} \omega_{SS}^{D_{HH}} \omega_{SI}^{D_{HI}} \omega_{II}^{D_{II}} \prod_{j=2}^n \left[\tilde{M}(t_j) (I_{p_{j1}}(t_j))^{F_j} \right] \\ &\quad \times \exp \left(- \int_0^{T_{\max}} [\beta SI(t) + \gamma I(t) + \tilde{\alpha}^T \mathbf{M}_{\max}(t) + (\tilde{\omega} - \tilde{\alpha})^T \mathbf{M}(t)] dt \right). \end{aligned} \quad (14)$$

Inference Given Complete Event Data The derived likelihood function in (14) indicates that inference should be relatively straightforward when all the changes in the process are fully observed. Given the complete event data $\{e_j\}_{j=1}^n$ and the initial conditions of the process \mathcal{G}_0 and $I(0)$, the only unknown quantities in (14) are the model parameters $\Theta = \{\beta, \gamma, \alpha_{SS}, \alpha_{SI}, \alpha_{II}, \omega_{SS}, \omega_{SI}, \omega_{II}\}$. In the following theorems, we state results on maximum likelihood estimation as well as Bayesian estimation.

Theorem 3.1 (Maximum likelihood estimation). *Following the likelihood function in (14), given \mathcal{G}_0 and complete event data $\{e_j\}$, the MLEs of the model parameters are given as follows:*

$$\begin{aligned} \hat{\beta} &= \frac{n_E - 1}{\sum_{j=1}^n SI(t_j)(t_j - t_{j-1})}, & \hat{\gamma} &= \frac{n_R}{\sum_{j=1}^n I(t_j)(t_j - t_{j-1})}, \\ \hat{\alpha}_{SS} &= \frac{C_{HH}}{\sum_{j=1}^n \left[\frac{H(t_j)(H(t_j)-1)}{2} - M_{HH}(t_j) \right] (t_j - t_{j-1})}, & \hat{\omega}_{SS} &= \frac{D_{HH}}{\sum_{j=1}^n M_{HH}(t_j)(t_j - t_{j-1})}, \\ \hat{\alpha}_{SI} &= \frac{C_{HI}}{\sum_{j=1}^n [H(t_j)I(t_j) - M_{HI}(t_j)] (t_j - t_{j-1})}, & \hat{\omega}_{SI} &= \frac{D_{HI}}{\sum_{j=1}^n M_{HI}(t_j)(t_j - t_{j-1})}, \\ \hat{\alpha}_{II} &= \frac{C_{II}}{\sum_{j=1}^n \left[\frac{I(t_j)(I(t_j)-1)}{2} - M_{II}(t_j) \right] (t_j - t_{j-1})}, & \hat{\omega}_{II} &= \frac{D_{II}}{\sum_{j=1}^n M_{II}(t_j)(t_j - t_{j-1})}. \end{aligned}$$

The above results can be directly obtained by setting all partial derivatives of the log-likelihood to zero. The detailed proof is provided in Supplement S2.

Theorem 3.2 (Bayesian inference with conjugate priors). *If Gamma priors are adopted for all the parameters:*

$$\beta \sim Ga(a_\beta, b_\beta), \quad \gamma \sim Ga(a_\gamma, b_\gamma), \quad \alpha_{..} \sim Ga(a_\alpha, b_\alpha), \quad \omega_{..} \sim Ga(a_\omega, b_\omega).$$

Then following the likelihood function in (14) and given \mathcal{G}_0 as well as the complete data $\{e_j\}$, the posterior distributions of the parameters are given by

$$\begin{aligned} \beta|\{e_j\} &\sim Ga(a_\beta + (n_E - 1), b_\beta + (n_E - 1)/\hat{\beta}), \quad \gamma|\{e_j\} \sim Ga(a_\gamma + n_R, b_\gamma + n_R/\hat{\gamma}), \\ \alpha_{SS}|\{e_j\} &\sim Ga(a_\alpha + C_{HH}, b_\alpha + C_{HH}/\hat{\alpha}_{SS}), \quad \omega_{SS}|\{e_j\} \sim Ga(a_\omega + D_{HH}, b_\omega + D_{HH}/\hat{\omega}_{SS}), \\ \alpha_{SI}|\{e_j\} &\sim Ga(a_\alpha + C_{HI}, b_\alpha + C_{HI}/\hat{\alpha}_{SI}), \quad \omega_{SI}|\{e_j\} \sim Ga(a_\omega + D_{HI}, b_\omega + D_{HI}/\hat{\omega}_{SI}), \\ \alpha_{II}|\{e_j\} &\sim Ga(a_\alpha + C_{II}, b_\alpha + C_{II}/\hat{\alpha}_{II}), \quad \omega_{II}|\{e_j\} \sim Ga(a_\omega + D_{II}, b_\omega + D_{II}/\hat{\omega}_{II}), \end{aligned} \quad (15)$$

where $\hat{\beta}, \hat{\gamma}, \hat{\alpha}_{SS}, \hat{\alpha}_{SI}, \hat{\alpha}_{II}, \hat{\omega}_{SS}, \hat{\omega}_{SI}, \hat{\omega}_{II}$ are the MLEs for the parameters defined in Theorem 3.1.

Note that (14) implies that each parameter is essentially the rate of Exponential wait times between consecutive events of a continuous-time Markov process. Applying the Gamma-Exponential conjugacy leads to the posterior distributions in (15).

Relaxing the closed population assumption Throughout this section, the host population is implicitly assumed to be closed. If, instead, the observed population is in fact a subset (with its size N still fixed) of a larger yet unobserved population, then it is possible for an individual to get infected by an external source that is not under study. This external infection force cannot be reflected by the per S - I link infection rate β , so we introduce an “external infection” rate ξ as the rate for each susceptible individual to contract the disease from an external source. ξ can also be thought of as the constant rate for every S individual to spontaneously enter status I , independently of the influence from the infected members inside the population. In this scenario the complete data likelihood becomes

$$\mathcal{L}(\beta, \xi, \gamma, \tilde{\alpha}, \tilde{\omega}|\mathcal{G}_0) = \gamma^{n_R} \alpha_{SS}^{C_{HH}} \alpha_{SI}^{C_{HI}} \alpha_{II}^{C_{II}} \omega_{SS}^{D_{HH}} \omega_{SI}^{D_{HI}} \omega_{II}^{D_{II}} \prod_{j=2}^n \left[\tilde{M}(t_j) (\beta I_{p_{j1}}(t_j) + \xi)^{F_j} \right]$$

$$\times \exp \left(- \int_0^{T_{\max}} [\beta SI(t) + \xi S(t) + \gamma I(t) + \tilde{\alpha}^T \mathbf{M}_{\max}(t) + (\tilde{\omega} - \tilde{\alpha})^T \mathbf{M}(t)] dt \right).$$

The MLEs for $\{\gamma, \tilde{\alpha}, \tilde{\omega}\}$ remain unchanged, and although there isn't a closed-form solution for the MLEs of β and ξ , numerical solutions can be easily obtained.

Moreover, if we have information on which infection cases are caused by internal sources (described by β) and which are caused by external sources (described by ξ), then we can directly obtain the MLEs and Bayesian posterior distributions for all the parameters, and estimation for all parameters except β and ξ remains unchanged. When there is missingness in recovery times, the Bayesian inference procedure proposed in the next section can still be carried out, with some minor adaptations. More details about inference with observations on an open population are included in Supplement S3.

4 Inference with Partial Epidemic Observations

Though likelihood-based inference is straightforward when all events are observed, complete event data are rarely collected in real-world epidemiological studies. Even in epidemiological studies with very comprehensive observations (e.g. the study by Aiello et al. (2016), in which individual social contacts were dynamically tracked using mobile devices), there still exists some degree of missingness in the exact individual recovery times. This is because infection times are reported when a study subject shows (and takes notice of) symptoms, but recoveries are almost never immediately recorded when a subject becomes disease-free.

Incomplete observations on epidemic paths have long been a major challenge for inference, even assuming a randomly mixing population or a simple, fixed network structure. With the exact times of infections and/or recoveries unknown, it essentially requires integrating over all possible individual disease episodes to obtain the marginal posterior distribution of the parameters. In most cases, this is intractable. Instead, one can bypass the marginalization through data augmentation: treat the unknown quantities in data as latent variables, iteratively impute or propose them, and then estimate parameters based on the likelihood function evaluated with the augmented, complete data. This class of methods have been developed for epidemic model inference based on individual-level data (Auranen et al., 2000;

Höhle and Jørgensen, 2002; Cauchemez et al., 2006; Hoti et al., 2009; Tsang et al., 2019), population-wide prevalence counts (Fintzi et al., 2017), and observations on a structured (but static) population (Neal and Roberts, 2004; O’Neill, 2009; Tsang et al., 2019), but has not yet been designed for an epidemic process coupled with a *dynamic* network. The time-varying nature of social interactions imposes complex constraints on the implementation of data augmentation, which already involves difficult conditioned sampling, so previous techniques can be quite ineffective or inefficient. Yet, network dynamics also provides information on possible infection sources and transmission routes that should be exploited.

In this section, we derive a data augmentation method specifically designed to enable inference under missing recovery times. The algorithm utilizes the information presented by the dynamic contact structure. In contrast to existing methods (such as Fintzi et al. (2017) and Hoti et al. (2009)), it is able to efficiently impute unobserved event times in parallel instead of updating individual trajectories one by one.

4.1 Method Overview

Problem setting Our goal is to conduct inference despite the absence of exact times of recovery events in the observed data. Throughout the observation period $(0, T_{\max}]$, suppose $\{(u_\ell, v_\ell]\}_{\ell=1}^L$ ($u_\ell < v_\ell$ and $v_\ell \leq u_{\ell+1}$) is the collection of *disjoint* time intervals in which a certain number of recoveries occur, but the exact times of those recoveries are unknown. That is, for each $\ell = 1, 2, \dots, L$, some individuals are reported as infected up to time u_ℓ , and they are reported as healthy again starting from time v_ℓ . Within one particular interval $(u_\ell, v_\ell]$, let $n_E^{(\ell)}$ be the number of infections, and $n_R^{(\ell)}$ the number of recoveries for which the *exact times are known*, so the number of *unknown* recovery times for this interval is $R_\ell = I(u_\ell) - I(v_\ell) + n_E^{(\ell)} - n_R^{(\ell)}$. Label the R_ℓ individuals with unknown recovery times by $\{k_{\ell,1}, \dots, k_{\ell,R_\ell}\}$, and denote their recovery times by latent variables $\{r_{\ell,1}, \dots, r_{\ell,R_\ell}\}$.

Further assume that we have a health status report (indicating ill or healthy) of each individual periodically during $(0, T_{\max}]$. Access to such information is usually granted in epidemiological studies where every study subject gives updates on health statuses through regular surveys (for example, weekly surveys).

Inference scheme We propose to address the problem of missing recovery times through data-augmented Markov chain Monte Carlo sampling. Given the observed data $\mathbf{x} = \{e_j\} \cup \{\text{health status reports}\} \cup \mathcal{Z}_0$ and an initial guess of parameter values $\Theta^{(0)}$, the algorithm iteratively samples a set of values for the missing recovery times $\{r_{\ell,1}, \dots, r_{\ell,R_\ell}\}_{\ell=1:L}^{(s)}$ from their probability distribution conditioned on \mathbf{x} and the current draw of parameter values, and then samples a new set of parameter values $\Theta^{(s)}$ from their posterior distributions conditioned on the augmented, complete data.

Let S be the maximum number of iterations, then for $s = 1 : S$, do:

1. **Data augmentation.** For $\ell = 1 : L$, draw $\{r_{\ell,i}^{(s)}\}_{i=1:R_\ell}$ from their joint conditional distribution

$$p(\{r_{\ell,i}\}_{i=1:R_\ell} | \Theta^{(s-1)}, \mathbf{x}, \{r_{\ell',i}\}_{i=1:R_{\ell'}, \ell' \neq \ell}). \quad (16)$$

2. **Update parameter values.** Combine \mathbf{x} and $\{r_{\ell,i}^{(s)}\}_{i=1:R_\ell, \ell=1:L}$ to form the augmented, complete data. Sample parameters $\Theta^{(s)}$ according to (15).

4.2 Data Augmentation via Endpoint-conditioned Sampling

In the inference scheme stated above, the data augmentation step (step 1) is challenging. This is because (16) describes the distribution of missing recovery times conditioned on both historical events *and* future events, and thus sampling from (16) is in fact sampling unobserved event times from a continuous-time Markov process with a series of fixed endpoints (Hobolth and Stone, 2009). Even though (3) suggests that, in *forward simulations*, the time it takes for an infected person to recover only depends on the recovery rate γ and is completely independent of the individual's social links or the epidemic history of any other individual, when recovery times need to be inferred *retrospectively*, there are additional constraints imposed by the observed data. First of all, an individual q cannot recover before a certain time point t if it is observed that at time t the person is still ill. Second, and more subtly, if another individual p gets infected during his contact with q , then q shouldn't have a recovery time that leaves p without any possible infection source. The first condition is easy to satisfy. The second constraint, in comparison, is much more complicated due to the network dynamics, which a simple forward simulation approach would fail to effectively

accommodate.

We tackle the challenge in data augmentation by first simplifying the expression of (16) and then stating an efficient sampling algorithm.

Lemma 4.1. (16) can be simplified into the following expression:

$$p\left(\{r_{\ell,i}\}_{i=1:R_\ell}|\gamma^{(s-1)}, \{e_j\}_{t_j \in (u_\ell, v_\ell]}, \mathcal{Z}_{u_\ell}\right), \quad (17)$$

where \mathcal{Z}_t is the state of the process at time t , including the epidemic status of each individual and the social network structure.

Proof. Consider the joint density of the complete data given parameter values $\Theta^{(s-1)}$.

$$\begin{aligned} & p(\mathbf{x}, \{r_{\ell,i}\}_{i=1:R_\ell, \ell=1:L} | \Theta^{(s-1)}) \\ &= \prod_{\ell=1:L} \left[p(\{e_j\}_{t_j \in (u_\ell, u_{\ell+1}]}, \{r_{\ell,i}\}_{i=1:R_\ell} | \mathcal{Z}_{u_\ell}, \Theta^{(s-1)}) \right] \times p(\{e_j\}_{t_j \leq u_1 \text{ or } t_j > v_L} | \mathcal{Z}_0, \mathcal{Z}_{v_L}, \Theta^{(s-1)}) \\ &= \prod_{\ell=1:L} \left[p(\{e_j\}_{t_j \in (u_\ell, v_\ell]} | \{r_{\ell,i}\}_{i=1:R_\ell}, \mathcal{Z}_{u_\ell}, \Theta^{(s-1)}) p(\{r_{\ell,i}\}_{i=1:R_\ell} | \mathcal{Z}_{u_\ell}, \gamma^{(s-1)}) \right] \\ & \quad \times \left[\prod_{\ell=1:L} p(\{e_j\}_{t_j \in (v_\ell, u_{\ell+1}]} | \mathcal{Z}_{v_\ell}, \Theta^{(s-1)}) \right] p(\{e_j\}_{t_j \leq u_1 \text{ or } t_j > v_L} | \mathcal{Z}_0, \mathcal{Z}_{v_L}, \Theta^{(s-1)}). \end{aligned}$$

Examining all terms concerning $\{r_{\ell,i}\}_{i=1:R_\ell}$ for each ℓ leads to

$$p(\{r_{\ell,i}\}_{i=1:R_\ell} | \Theta^{(s-1)}, \mathbf{x}, \{r_{\ell',i}\}_{i=1:R_{\ell'}, \ell' \neq \ell}) = p(\{r_{\ell,i}\}_{i=1:R_\ell} | \gamma^{(s-1)}, \{e_j\}_{t_j \in (u_\ell, v_\ell]}, \mathcal{Z}_{u_\ell}).$$

□

The lemma above suggests that imputation of missing recovery times inside an interval $(u, v]$ only depends on the events that occur in $(u, v]$, the state of the process at the start of the interval, \mathcal{Z}_u , and the value of recovery rate γ .

Now consider sampling recovery times within any interval $(u, v]$. Let \mathcal{Q} denote the group of individuals who recover at unknown times during $(u, v]$, and for each $q \in \mathcal{Q}$, let q 's exact recovery time be $r_q \in (u, v]$. Similarly, let \mathcal{P} denote the group of individuals who get infected during $(u, v]$; for $p \in \mathcal{P}$, let p 's infection time be i_p , $\mathcal{N}_p(i_p)$ be the set of p 's contacts at time i_p , and $\mathcal{I}(i_p)$ be the set of *known* infected individuals at time i_p (that is, $\mathcal{I}(i_p)$ excludes any individual who may have recovered before i_p).

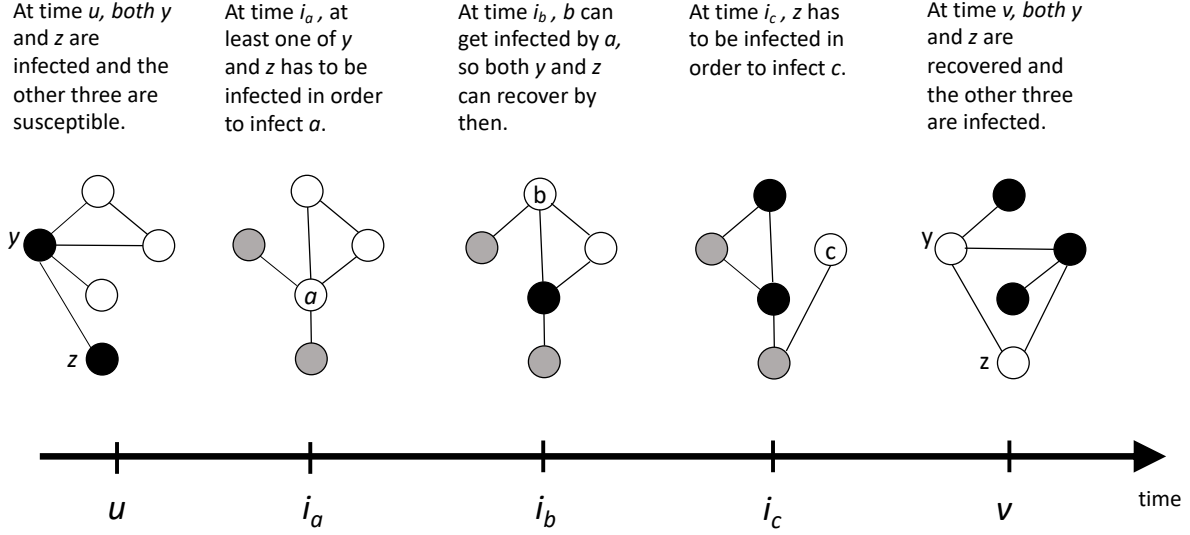


Figure 1: Illustration of the DARCI data augmentation algorithm, on a population of size $N = 5$. Each circle represents an individual and each solid line represents a link. Disease status is color coded: dark = infected, grey = unknown (possibly infected or recovered), and white = healthy (susceptible or recovered). Individuals y and z are known to be infectious at time u but are recovered by time v , and individuals a , b and c are known to get infected at time points i_a , i_b and i_c , respectively. For each person $p \in \{a, b, c\}$, the DARCI algorithm inspects p 's contacts at infection time i_p , and if the infectious contacts consist only of y and/or z , then y or z 's recovery has to occur after time i_p .

Proposition 4.2 (Data augmentation regulated by contact information (DARCI)). *Following the notation stated above, given a recovery rate γ , the state of the process at time u , \mathcal{Z}_u , and all the observed events in the interval $(u, v]$, $\{e_j\}_{t_j \in (u, v]}$, one can sample $\{r_q\}$ from the conditional distribution $p(\{r_q\} | \gamma, \{e_j\}_{t_j \in (u, v]}, \mathcal{Z}_u)$ in the following steps:*

1. Initialize a vector LB of length $|\mathcal{Q}|$ with $LB_q = u$ for every $q \in \mathcal{Q}$;
2. Arrange the set \mathcal{P} in the order of $\{p_1, p_2, \dots, p_{|\mathcal{P}|}\}$ such that $i_{p_1} < i_{p_2} < \dots < i_{p_{|\mathcal{P}|}}$, and for each $p \in \mathcal{P}$ (chosen in the arranged order), examine the set

$$\mathcal{I}_p = (\mathcal{N}_p(i_p) \cup \{p\}) \cap (\text{Inf}(i_p) \cup \mathcal{Q}).$$

If $\mathcal{I}_p \subset \mathcal{Q}$, then randomly and uniformly select one $q \in \mathcal{I}_p$, and set $LB_q = i_p$.

3. Draw recovery times $r_q \stackrel{\text{ind}}{\sim} \text{TEXP}(\gamma, LB_q, v)$, where $\text{TEXP}(\gamma, s, t)$ is a truncated Exponential distribution with rate γ and truncated on the interval (s, t) .

The intuition is to draw a sample of recovery times that are “consistent with” the observed data. To achieve this goal, an imputed recovery cannot occur in a way that leaves a to-be-infected individual without any infectious neighbor at the time of infection, nor take place before the corresponding individual gets infected. Effectively there is a “lower bound” for each missing recovery time conditioned on the observed data, particularly the dynamic contact structure. An illustration of the DARCI algorithm is provided in Figure 1.

Combining Lemma 4.1 and Proposition 4.2 enables exact sampling from the conditional distribution (17) in the data augmentation step: for each $\ell = 1, 2, \dots, L$, applying the DARCI algorithm to the interval $(u_\ell, v_\ell]$ gives an updated set of missing recovery times, $\{r_{\ell,i}\}_{i=1:R_\ell}$. This makes the MCMC sampling scheme simply a Gibbs sampler.

5 Simulation Experiments

In this section we present results of a series of experiments with simulated datasets. In all experiments, we employ a forward simulation procedure that can be seen as a variation of Gillespie’s algorithm (Gillespie, 1976) in order to generate realizations of the dynamic network epidemic process. The input consists of the parameter values $\Theta = \{\beta, \gamma, \tilde{\alpha}, \tilde{\omega}\}$ ², an arbitrary initial social network \mathcal{G}_0 , the number of infectious cases at onset $I(0)$, and the maximum observation time T_{\max} . The output is the complete collection of all the events that occur within the time interval $(0, T_{\max}]$, $\{e_j = (t_j, p_{j1}, p_{j2}, F_j, C_j, D_j)\}$, and for each event e_j , there is a timestamp (t_j) , labels of the individuals involved (p_{j1}, p_{j2}) , and the type of the event (indicated by F_j, C_j, D_j).

The steps of the simulation procedure are detailed as follows:

1. **Initialization.** Randomly select $I(0)$ individuals to be the infected/infectious (then the rest of the population are all susceptible). Set $t_{\text{cur}} = 0$.
2. **Iterative update.** While $t_{\text{cur}} < T_{\max}$, do:

²Here $\tilde{\alpha} = (\alpha_{SS}, \alpha_{SI}, \alpha_{II})^T$ and $\tilde{\omega} = (\omega_{SS}, \omega_{SI}, \omega_{II})^T$, as defined in (10) and (11).

- (a) **Bookkeeping.** Summarize the following statistics at t_{cur} : 1) $SI(t_{\text{cur}})$, the number of S-I links in the population; 2) $\mathbf{M}_{\text{max}}(t_{\text{cur}})$, the possible number of links of each type defined in (12); 3) $\mathbf{M}(t_{\text{cur}})$, the number of existing links of each type defined in (13). Then set $\mathbf{M}^d(t_{\text{cur}}) = \mathbf{M}_{\text{max}}(t_{\text{cur}}) - \mathbf{M}(t_{\text{cur}})$.
- (b) **Next event time.** Compute the instantaneous rate of the occurrence of any event, $\Lambda(t_{\text{cur}}) = \beta SI(t_{\text{cur}}) + \gamma I(t_{\text{cur}}) + \tilde{\alpha}^T \mathbf{M}^d(t_{\text{cur}}) + \tilde{\omega}^T \mathbf{M}(t_{\text{cur}})$, and draw $\Delta t \sim \text{Exponential}(\Lambda(t_{\text{cur}}))$.
- (c) **Next event type.** Sample $Z \sim \text{Multinomial}(\tilde{\lambda}(t_{\text{cur}}))$, where

$$\tilde{\lambda}(t_{\text{cur}}) = \left(\frac{\beta SI(t_{\text{cur}})}{\Lambda(t_{\text{cur}})}, \frac{\gamma I(t_{\text{cur}})}{\Lambda(t_{\text{cur}})}, \frac{\tilde{\alpha}^T \mathbf{M}^d(t_{\text{cur}})}{\Lambda(t_{\text{cur}})}, \frac{\tilde{\omega}^T \mathbf{M}(t_{\text{cur}})}{\Lambda(t_{\text{cur}})} \right)^T.$$

Then do one of the following based on the value of Z :

If $Z = 1$ (infection), uniformly pick one S - I link and infect the S individual in this link.

If $Z = 2$ (recovery), uniformly pick one I individual to recover.

If $Z = 3$ (link activation), randomly select $Y \in \{\text{H-H}, \text{H-I}, \text{I-I}\}$ with probabilities proportional to $\tilde{\alpha} \circ \mathbf{M}^d(t_{\text{cur}})$, and uniformly pick one de-activated “ Y link” to activate.

If $Z = 4$ (link termination), randomly select $Y \in \{\text{H-H}, \text{H-I}, \text{I-I}\}$ with probabilities proportional to $\tilde{\omega} \circ \mathbf{M}(t_{\text{cur}})$, and uniformly pick one existing “ Y link” to terminate.

- (d) Replace t_{cur} by $t_{\text{cur}} + \Delta t$, record relevant information about the sampled event, and repeat from (a).

In Step 2 (c), “ \circ ” refers to the Hadamard product (entrywise product) for two vectors.

5.1 Experiments with Complete Observations

In this subsection, we first demonstrate the insufficiency of analyzing disease spread without considering the network structure or its dynamics. Then we validate our claims on maximum likelihood estimation and Bayesian inference given complete event data (Theorems 3.1 and 3.2). Finally, we show that the model estimators can detect simpler models such as the decoupled process and the static network process.

Unless otherwise stated, we set the initial network \mathcal{G}_0 as a random Erdős–Rényi graph (undirected) with edge probability $p = 0.1$, let $I(0) = 1$ individual to be infected at onset, and choose the ground-truth parameters as

$$\beta = 0.03, \gamma = 0.12; \tilde{\alpha}^T = (0.005, 0.001, 0.005), \tilde{\omega}^T = (0.05, 0.1, 0.05). \quad (18)$$

For Bayesian inference, we adopt the following Gamma priors for the parameters ³:

$$\beta \sim Ga(1, 1/0.02), \gamma \sim Ga(1, 1/0.1); \alpha_{..} \sim Ga(1, 1/0.004), \omega_{..} \sim Ga(1, 1/0.06). \quad (19)$$

For each parameter, 1000 posterior samples are drawn after a 200-iteration burn-in period.

The danger of neglecting networks or network dynamics Adopting the “random mixing” assumption about an actually networked population can lead to severe underestimation of the infection rate. Erroneous estimation can also happen if contacts are in fact dynamic but are mistaken as static during inference. Table 2 displays the MLEs of the infection rate β (**true value 0.05**) obtained by methods under three different assumptions regarding the network structure (assuming a dynamic network, assuming a static network, and assuming random mixing without any network). The population size is $N = 50$, and results are summarized over 50 different simulated datasets.

These results make clear that neglecting the constraints of social networks, even when the quantity of interest is the disease transmission rate, is dangerously misleading, producing estimates that are not at all close to the truth. While incorporating the initial network structure statically throughout the process helps (note that the 95% confidence interval does include the truth), disregarding the evolution of the network over time is still a significant model misspecification and leads to biases.

³Note that the prior means are different from the true parameter values, and experiments show that results are in fact insensitive to prior specifications as long as a reasonable amount of data is available.

Table 2: Maximum likelihood estimates of β , the per link infection rate (real value 0.05), using dynamic network information, the initial static network structure, and no network structure at all (assuming random mixing), respectively. The standard deviations as well as the 2.5% and 97.5% quantiles of the estimates are obtained from outcomes across 50 different simulated datasets on a $N = 50$ population.

Method	dynamic network	static network	no network
Estimate	0.0540	0.0278	0.00219
Standard deviation	0.0158	0.0081	0.000821
2.5% quantile	0.0230	0.00825	0.000614
97.5% quantile	0.0817	0.0553	0.00425

Validity and effectiveness of parameter estimation Complete event data are generated using the simulation procedure stated in above, and maximum likelihood estimates (MLEs) as well as Bayesian estimates are obtained for parameters $\Theta = \{\beta, \gamma, \tilde{\alpha}, \tilde{\omega}\}$. Here we set the population size as $N = 100$ and the infection rate as $\beta = 0.03$.

Figure 2 shows the results of maximum likelihood estimation in one simulated dataset. The MLEs for the each parameter (dark solid line) are computed using various numbers of events, and are compared with the true parameter value (red horizontal lines). The lower and upper bounds for 95% confidence intervals are also calculated (dashed gray lines). Only the MLEs for parameters $\beta, \gamma, \alpha_{SS}$ and α_{SI} are shown, but results for all parameters are included in Supplement S4. Estimation is relatively accurate even when observation ends earlier than the actual process (thus leaving later events unobserved). When more events are available for inference, accuracy is improved and the uncertainty is reduced.

Figure 3 presents the posterior sample means (solid lines) and 95% credible bands (shades) for each parameter inferred using various numbers of events, with the true parameter values marked by bold, dark horizontal lines. The results are shown for 4 different simulated datasets (each dataset represented by a distinct color) and for parameters $\beta, \gamma, \omega_{SS}$ and ω_{SI} (complete results are in Supplement S4). When more events are utilized in inference, the posterior means tend to be closer to the true parameter values, while the credible bands

gradually narrow down.

It is worth noting that parameter estimation is unaffected by either the population size N or the initial network structure \mathcal{G}_0 . In particular, the model is capable of handling large-scale networks as well as arbitrary network structures. Additional results with larger values of N and different configurations of \mathcal{G}_0 are provided in Supplement S4.

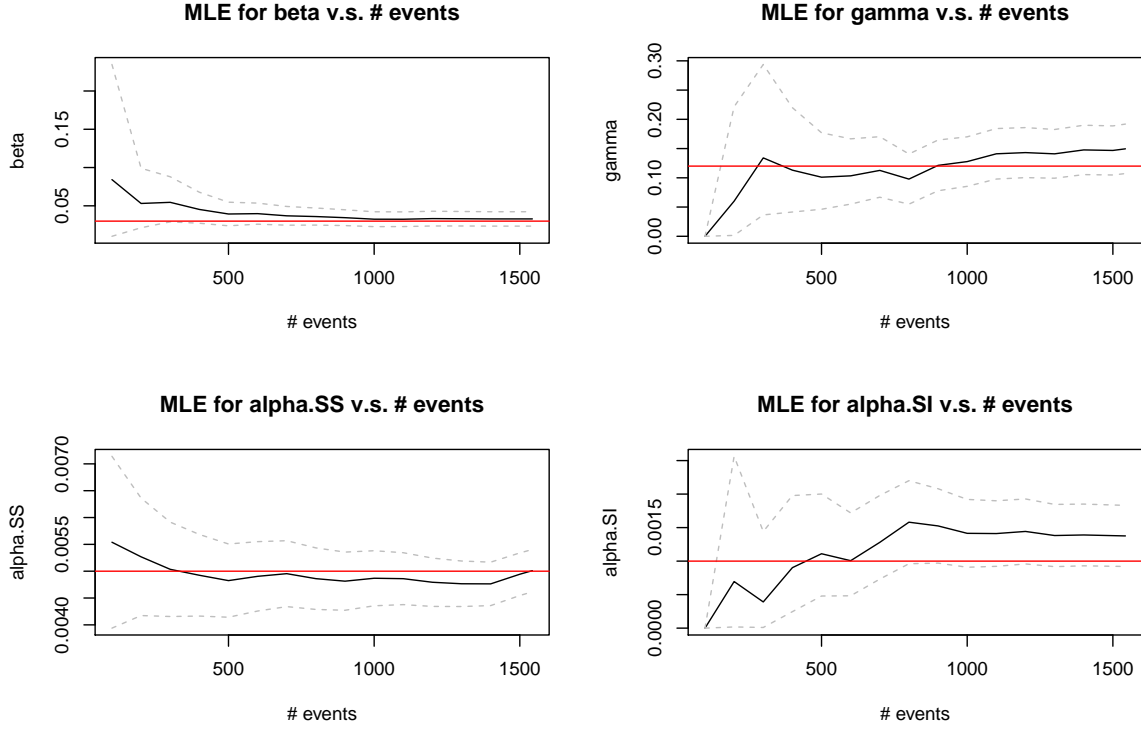


Figure 2: MLEs versus number of events used for inference. Dashed gray lines show the lower and upper bounds for 95% frequentist confidence intervals, and red lines mark the true parameter values. Results are presented for $\beta, \gamma, \alpha_{SS}$ and α_{SI} .

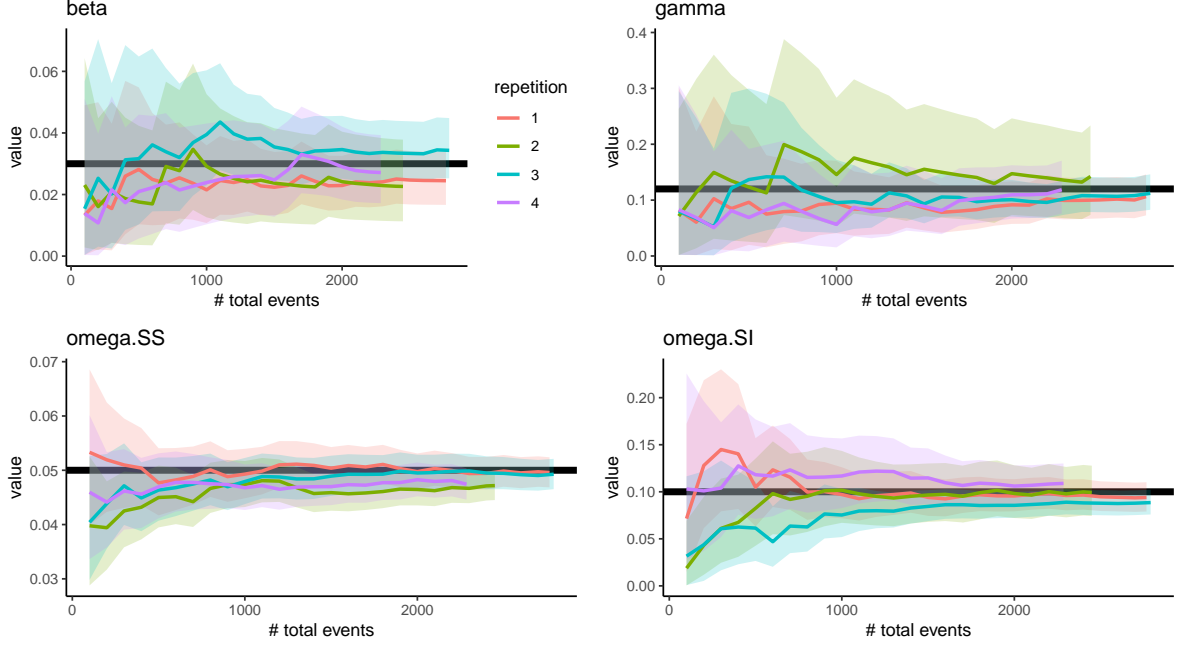


Figure 3: Posterior sample means versus number of total events used for inference. True parameter values are marked by **bold dark** horizontal lines, along with 95% credible bands. Results are presented for 4 different complete datasets and for parameters $\beta, \gamma, \omega_{SS}$ and ω_{SI} .

Assessing model flexibility Our proposed model is a generalization of temporal network epidemic processes where the network evolves independently of the contagion (the “decoupled” process), which in turn is a generalization of epidemic processes on static networks (the “static network” process). Therefore, if a set of events is actually generated from the decoupled process, then we expect all the link activation and termination rates to be estimated as the same. Likewise, if the events are generated from the static network process, then we expect all the link rates to be estimated as zero.

To confirm this, experiments are conducted on complete event datasets generated using the two simpler models. Here we only show select results of Bayesian inference on datasets generated from static network epidemic processes (Figure 4) and delegate other results to Supplement S4. We can see that information about a moderate number of events is sufficient to accurately estimate the epidemic-related parameters (β and γ) and uncover the static nature of the network; note how quickly the posterior credible bands for α_{SI} and ω_{SI} shrink toward zero.

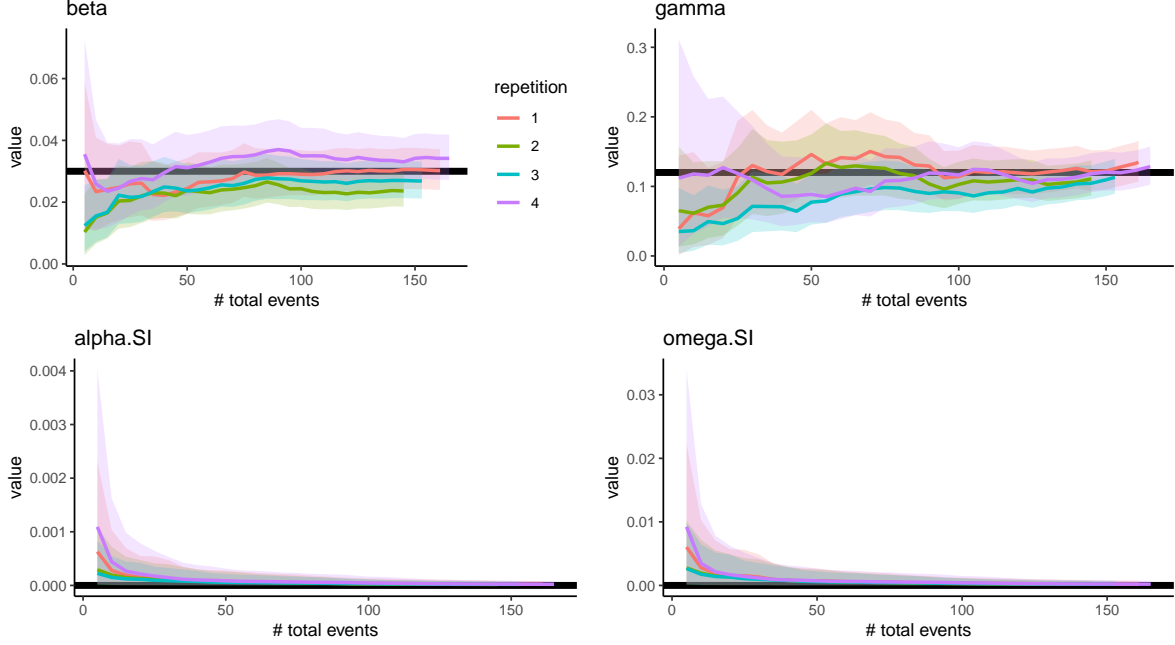


Figure 4: Posterior sample means versus number of total events used for inference, with data generated from *static* network epidemic processes. True parameter values are marked by **bold dark** horizontal lines, along with 95% credible bands. Results are presented for 4 different complete datasets and for parameters $\beta, \gamma, \alpha_{SI}$ and ω_{SI} . With a moderate number of events, the epidemic-related parameters, β and γ , are accurately estimated, and the posteriors for the edge rates quickly shrink toward zero (the truth).

5.2 Experiments with Incomplete Observations

Upon validating the model and inference framework in the previous subsection, we are now ready to assess the performance of our proposed inference scheme in the more realistic setting where epidemic observations are incomplete. In this subsection, we first verify that the MCMC sampling scheme in Section 4 is able to retrieve the parameter values despite the unavailability of exact recovery times in the observed data. Then we compare our DARCI algorithm (Prop. 4.2) with two baselines and show that it produces posterior samples of higher quality and with higher efficiency.

Simulating partially observed data We first generate complete event data using the simulation procedure stated earlier in this section, and then randomly take out $\eta \times 100\%$

of the recovery times and treat them as unknown. Meanwhile, a disease status report (as described in Section 4.1) is produced every 7 time units throughout the entire process. Note that the scale of time is insignificant here—the physical length τ of 1 time unit can be thought of as a second, an hour, or a day, since τ only determines how we *interpret* the parameters (which govern how fast the system evolves per unit time) but not the realization of the process. Therefore, we can regard 1 time unit as *a day*, and the periodical disease status report as a *weekly* report.

Efficacy of the inference scheme We demonstrate the efficacy of the inference scheme outlined in Section 4.1 through experiments on an example dataset, where the settings and parameters are the same as those in (18) and the population size is fixed at $N = 100$. In this particular realization, there are 26 infection cases spanning over approximately 37 days (less than 6 weeks), and there are 767 and 893 instances of social link activation and termination, respectively.⁴

First set $\eta = 50$, that is, randomly select 50% of recovery times to be taken as missing. Figure 5 plots, for each parameter in $\{\beta, \gamma, \alpha_{SS}, \omega_{SS}\}$, 1000 consecutive MCMC samples (after a 200-iteration burn-in), as well as the 2.5% and 97.5% quantiles of the posterior samples (gray, dashed lines), compared with the true parameter value (red horizontal line). We can see that for every parameter, the 95% sample credible interval covers the true parameter value, suggesting that the proposed inference scheme is able to estimate parameters from incomplete data reasonably well.

Then set $\eta = 100$, which implies that all the recovery times are unknown. Figure 6 presents outcomes of the inference algorithm in this case. Understandably, parameter estimation is affected by the total unavailability of exact recovery times, but the drop in accuracy is marginal. Moreover, the credible bands are slightly wider, suggesting an increased uncertainty with more missingness.

⁴The event time scales in the example dataset are chosen to be comparable to, though not exactly the same as, those in the real-world data used in Section 6.

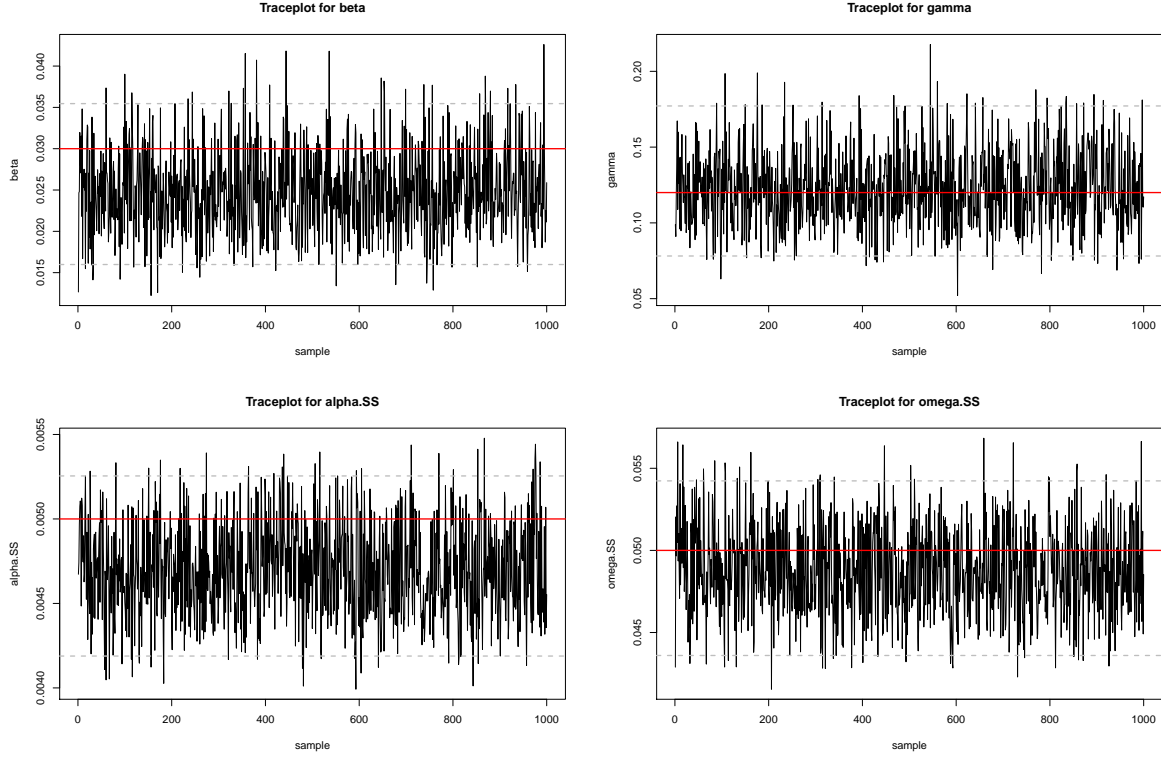


Figure 5: Inference results for parameters $\beta, \gamma, \alpha_{SS}, \omega_{SS}$ with 50% recovery time missingness. The uncertainty in exact recovery times does affect the estimation of the type-dependent edge rates, but not detrimentally (all the true parameter values fall into the 95% credible intervals of the posteriors).

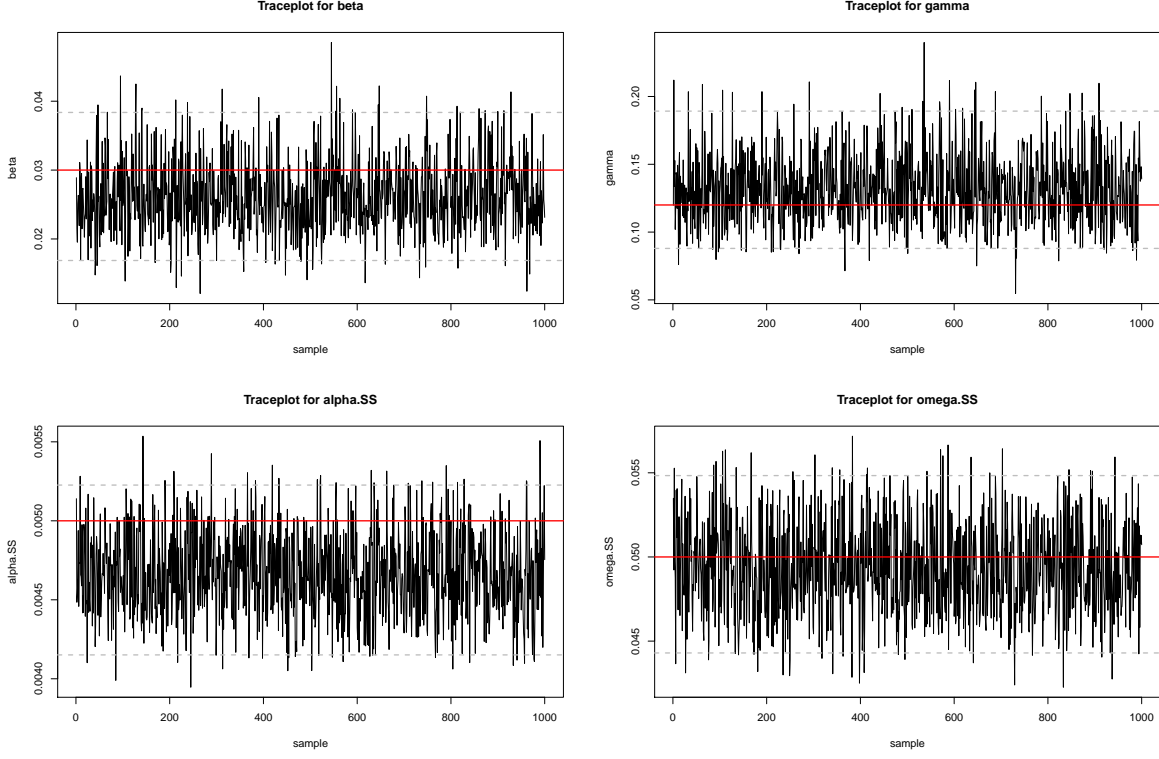


Figure 6: Inference results for parameters $\beta, \gamma, \alpha_{SS}, \omega_{SS}$ with complete (100%) missingness in recovery times. Still, all the true parameter values fall into the 95% credible intervals of the posteriors, suggesting the capability of the inference algorithm to estimate parameters even when there is considerable uncertainty in individual epidemic histories.

Efficiency of the DARCI algorithm We test the performance of the data augmentation algorithm stated in Proposition 4.2 by comparing it with two other more conventional sampling methods:

1. **Rejection sampling:** Carry out Step 1 of the inference scheme via rejection sampling. For $\ell = 1 : L$, keep proposing recovery times $\{r_{\ell,i}^*\}_{i=1:R_\ell} \stackrel{iid}{\sim} \text{TEXP}(\gamma^{(s-1)}, u_\ell, v_\ell)$ until the proposed $\{r_{\ell,i}^*\}_{i=1:R_\ell}$ are compatible with the observed event data in $(u_\ell, v_\ell]$. We label this method by “**Reject**”.
2. **Metropolis-Hastings:** Modify Step 1 of the inference scheme into a Metropolis-Hastings step. For $\ell = 1 : L$, propose recovery times $\{r_{\ell,i}^*\}_{i=1:R_\ell} \stackrel{iid}{\sim} \text{TEXP}(\gamma^{(s-1)}, u_\ell, v_\ell)$,

and accept them as $\{r_{\ell,i}^{(s)}\}_{i=1:R_\ell}$ with probability

$$\min \left(1, \frac{p(\mathbf{x}, \{r_{\ell,i}^*\}_{i=1:R_\ell}, \{r_{\ell',i}^{(s-1)}\}_{i=1:R_{\ell'}, \ell' \neq \ell} | \Theta^{(s-1)}) \text{pTEXP}(\{r_{\ell,i}^{(s-1)}\}_{i=1:R_\ell}; \gamma^{(s-1)}, u_\ell, v_\ell)}{p(\mathbf{x}, \{r_{\ell,i}^{(s-1)}\}_{i=1:R_\ell, \ell=1:L} | \Theta^{(s-1)}) \text{pTEXP}(\{r_{\ell,i}^*\}_{i=1:R_\ell}; \gamma^{(s-1)}, u_\ell, v_\ell)} \right),$$

which equals to 1 when the proposed $\{r_{\ell,i}^*\}_{i=1:R_\ell}$ are consistent with the observed event data in $(u_\ell, v_\ell]$ and 0 otherwise. If the proposal is not accepted, then set $\{r_{\ell,i}^{(s)}\}_{i=1:R_\ell} = \{r_{\ell,i}^{(s-1)}\}_{i=1:R_\ell}$. We label this method by “**MH**”.

Note that, the “**MH**” method employs the same principle as existing agent-based data augmentation methods (Cauchemez et al., 2006; Hoti et al., 2009; Fintzi et al., 2017) that propose candidates of individual disease histories and accept them with probabilities computed through evaluating the likelihood (or an approximation of it) and the proposal density. But in “**MH**” the implementation is actually simpler and computationally lighter, because the proposal is conditioned on known infection times and the current posterior draw of γ . The acceptance step is reduced to inspecting compatibility with known data, thus avoiding the intensive computation of likelihood evaluation.

Although the three methods give the same inference results since they all sample from the same posterior distributions, our data augmentation algorithm (labeled by “**DARCI**”) is more efficient than the other two in two aspects. First, since we draw a new sample of recovery times from the conditional distribution in (16) in every iteration, there is lower autocorrelation in the resulting Markov chain, which leads to better mixing and fewer iterations needed to achieve a certain effective sample size (especially so when compared with “**MH**”). Second, the DARCI algorithm is generally much less time consuming when drawing from the conditional distribution in (16) compared to “**Reject**”, because it parses out a configuration of “lower bounds” for imputing missing recovery times while accounting for the constraints imposed by contagion spreading and the dynamics of social links.

Three MCMC samplers are run using the three methods respectively on the dataset showcased above. In each sampler, 1000 consecutive samples are retained for each parameter after a 200-iteration burn-in period. For the resulting chain of each parameter, we calculate the effective sample size (ESS), the Geweke Z-score (Geweke et al., 1991), and the two-sided p-value for the Z-score. The results are presented in Table 3. Among the three

methods, “**MH**” suffers the most from the correlation between two successive samples, while “**DARCI**” seems to produce high-quality MCMC samples.

Table 3: MCMC diagnostics for three data augmentation sampling methods, labelled as “**DARCI**”, “**Reject**”, and “**MH**”. “ESS” stands for “effective sample size”. The “Z-score” is the test statistic for MCMC convergence proposed by Geweke et al. (1991), and the two-sided p-value for each standard Z-score is also computed. Samples acquired by **MH** tend to have higher auto-correlations and thus smaller effective sample sizes.

Statistic	β	γ	α_{SS}	α_{SI}	α_{II}	ω_{SS}	ω_{SI}	ω_{II}	Method
ESS	1000.00	1000.00	1000.00	1000.00	1000.00	1000.00	1000.00	1000.00	DARCI
Z-score	-0.90	-0.20	-0.56	-1.32	-0.22	0.84	-0.02	-1.24	
$Pr(> Z)$	0.37	0.84	0.58	0.19	0.82	0.40	0.99	0.22	
ESS	1000.00	1160.17	1000.00	955.29	1000.00	1000.00	926.63	1000.00	Reject
Z-score	0.48	-1.01	0.44	0.28	1.08	-2.18	-0.16	0.31	
$Pr(> Z)$	0.63	0.31	0.66	0.78	0.28	0.03	0.87	0.76	
ESS	566.43	1000.00	1000.00	1000.00	538.12	907.14	729.33	1000.00	MH
Z-score	-1.25	-1.83	-0.48	-0.59	-2.09	-0.24	-1.52	-0.57	
$Pr(> Z)$	0.21	0.07	0.63	0.55	0.04	0.81	0.13	0.57	

We then compare “**DARCI**” and “**Reject**” in their running times (see Table 4). A dataset is simulated where there are different numbers of recoveries with unknown times within 5 time intervals. The two sampling methods are applied to draw a set of recovery times for each of those 5 intervals, and over multiple runs, the minimum and median times they take are recorded. Although the two methods draw samples from the same conditional distribution, “**DARCI**” tends to take less time than “**Reject**” in one iteration.

Table 4: Comparison between the two sampling methods (“**DARCI**” and “**Reject**”) for imputing missing recovery times. Overall, the DARCI algorithm is more efficient, especially when the number of missing recovery times is relatively large (e.g. Interval 3), or there are special constraints on viable recovery times (e.g. Interval 1, where the observed events suggest that the recovery cannot occur until half way through the time interval).

Interval	#(To recover)	Min Time		Median Time	
		Reject	DARCI	Reject	DARCI
1	1	227 μ s	224 μ s	484 μ s	245 μ s
2	8	285 μ s	287 μ s	563 μ s	319 μ s
3	15	163 μ s	161 μ s	279 μ s	181 μ s
4	2	138 μ s	138 μ s	153 μ s	156 μ s
5	1	133 μ s	133 μ s	146 μ s	147 μ s

6 Influenza-like-illnesses on A University Campus

In this section, we apply the proposed model and inference scheme to a real-world dataset on the transmission of influenza-like illnesses among students on a university campus.

6.1 Data Overview

The data we analyze in this section were collected in a 10-week network-based epidemiological study, eX-FLU (Aiello et al., 2016). The study was originally designed to investigate the effect of social intervention on respiratory infection transmission. 590 university students enrolled in the study and were asked to respond to weekly surveys on influenza-like illness (ILI) symptoms and social interactions. 103 individuals further participated in a sub-study in which each study subject was provided a smartphone equipped with an application, iEpi. The application pairs smartphones with other nearby study devices via Bluetooth, recording individual-level social interactions at five-minute intervals.

The sub-study using iEpi was carried out from January 28, 2013 to April 15, 2013 (from week 2 until after week 10). Between weeks 6 and 7, there was a one-week spring break

(March 1 to March 7), during which the volume of recorded social contacts dropped noticeably. In our experiments, we use data collected on the $N = 103$ sub-study participants from January 28 to April 4 (week 2 to week 10), and treat the two periods before and after the spring break as two separate and independent observation periods ($T_{\max} = 31$ days for period 1 and $T_{\max} = 28$ days for period 2).

We take an infection event as the occurrence of a positive ILI case, and define a recovery event as the end of an individual’s flu-like symptoms (with the exact time unknown). A link between two study subjects is activated when the iEpi application registers the initial pairing of their smartphones, and the link is terminated when the Bluetooth detection stops. Altogether, the data contain 24 infection events in total (the exact times are known), with 14 before the spring break week and 10 after, as well as 45,760 social link activation and termination events. The weekly health status (healthy or ill) of every participant is acquired from the weekly surveys, so we know which individuals recovered during each particular week, but the exact recovery times are unknown. Summary statistics of the data are provided in Table 5. Overall, infection instance counts peaked in the middle of each observation period and dropped at the end, and the dynamic social network was quite sparse; more activity (in both the epidemic process and network process) was observed in the weeks before the spring break. Further details on data cleaning and pre-processing are provided in Supplement S5.

6.2 Analysis

Since the 103 individuals are sub-sampled from the 590 study participants, which are also sub-sampled from the entire population on the university campus, the real data are actually observed on an open population. Following the parameterization introduced at the end of Section 3.2, we include the parameter ξ to denote the rate of infection from an external source for each susceptible individual. Every infected individual that came into contact with any infectives within 3 days prior to the onset of symptoms is regarded as an internal case (governed by parameter β); otherwise the infection is labeled as an external case (governed by parameter ξ). This enables the inference procedure stated at the end of Section 4.

The data collected during the two observation periods are considered as separate and independent realizations of the same adaptive network epidemic processes. For each param-

Table 5: Summary statistics of the real data (processed) by week: number of new infection cases (top row), maximum network density (middle row), and minimum network density (bottom row). No new infection cases took place in week 2, but two participants were already ill at the beginning of the week. The dynamic network remained sparse throughout the duration of the sub-study, except for one instance in week 3—the unusually high network density only occurred on the night of February 4, possibly due to a large-scale on-campus social event.

Week	Wk 2	Wk 3	Wk 4	Wk 5	Wk 6
#(Infections)	0	3	5	4	2
Max. Density	0.0053	0.2048	0.0040	0.0038	0.0044
Min. Density	0.0000	0.0000	0.0000	0.0002	0.0000
Week	(break)	Wk 7	Wk 8	Wk 9	Wk 10
#(Infections)	N.A.	1	3	5	1
Max. Density	N.A.	0.0032	0.0032	0.0032	0.0023
Min. Density	N.A.	0.0000	0.0000	0.0000	0.0000

eter, samples drawn in the first 500 iterations are discarded and then every other sample is retained in the next 2000 iterations, resulting in 1000 posterior samples. Table 6 summarizes the posterior sample means and the lower and upper bounds of 95% sample credible intervals for a selection of parameters. The output from one chain is presented here; repeated runs (with different initial conditions and random seeds) yield similar results.

Our findings suggest that flu-like symptoms spread quite slowly but recoveries are made rather fast. On average, it takes about 14 days (2 weeks) of contact with one infectious person inside the population for a susceptible individual to start showing symptoms, yet it takes a little more than 3 days for someone to no longer feel ill. The external infection force is quite strong: given the number of susceptibles in the population (typically about 100), the population-wide external infection rate is approximately $100 \times 0.0033 = 0.33$, implying that an external ILI case is expected to occur every other three days. This is a reasonable estimate, since we observed 9 external infection cases within 28 days during the second observation period.

The inferred link rates reflect an interesting pattern in social interactions in this particular

Table 6: Posterior sample means and 95% credible intervals of select parameters obtained by the Bayesian inference scheme modified from that in Section 4. Inference is carried out jointly on the two periods before and after the spring break.

Parameter	Sample mean	2.5% quantile	97.5% quantile
β (internal infection)	0.0695	0.0247	0.1500
ξ (external infection)	0.00331	0.00208	0.00494
γ (recovery)	0.294	0.186	0.428
α_{SS} (S - S link activation)	0.0514	0.0499	0.0529
ω_{SS} (S - S link termination)	38.26	33.55	40.62
α_{SI} (S - I link activation)	0.130	0.0785	0.194
ω_{SI} (S - I link termination)	53.5	22.5	231.7

population: individuals are reluctant to establish contact and active contacts are broken off quickly—an average pair of healthy people initiate/restart their interaction after waiting 20 days and then end it after spending less than 40 minutes together. Moreover, it seems that on average a healthy-ill link is activated more frequently than a healthy-healthy link, but the former is also terminated faster—this might be because those students who fell ill in the duration of the study happen to be more socially proactive, but once their healthy social contacts realize they are sick and thus potentially infectious, the contact is cut short to avoid disease contraction.

It is also notable that the sample 95% credible intervals for β , α_{SI} and ω_{SI} are relatively wide, indicating a high level of uncertainty in the estimation for these parameters. It is challenging to estimate the internal infection rate β because dataset contains only 6 cases of internal infection in total (5 in period 1, 1 in period 2), providing limited information on the rate of transmission. Similar issues are present for the estimation of α_{SI} and ω_{SI} ; since there were no more than 5 infected individuals at any given time, network events related to them were few and far between. Moreover, since their exact recovery times are unknown, there is additional uncertainty associated with their exact disease statuses when they activated or terminated social links. Such measure of uncertainty, readily available through stochastic

modeling and Bayesian inference, provides valuable insights into the amount of information the data contain and the level of confidence we possess when making conclusions and interpretations. The inference outcomes imply that, for example, the real data sufficiently inform the contact patterns among healthy individuals in this population but are limited toward understanding how long a healthy person and a symptomatic person typically maintain their contact.

7 Discussion

This paper has focused on enabling inference for partially observed epidemic processes on dynamic and adaptive networks. We formulated a continuous-time Markov process model to describe the epidemic-network interplay and derived its complete data likelihood. This lead to the design of conditional sampling techniques that enable data augmented inference methods to accommodate missingness in individual recovery times.

The proposed framework for dynamic network epidemiology is a generalization and extension of previous methods. Certain concepts, such as infection and recovery rates, disease prevalence, and network density, are analogous to those in existing literature, and their interpretations are relatively straightforward from our generative, mechanistic model. Other concepts, however, are not readily transferable from more traditional settings to the adaptive network setting. One quantity of particular interest in most epidemiological models is the *basic reproductive number*, denoted by R_0 . It denotes the average number of secondary infections caused by a typical infectious individual at the early stage of the epidemic. Here, “early stage” refers to the initial period of the process during which only a negligible fraction of the entire population is infected, such that any person that comes into contact with an infected individual can be assumed to be susceptible. R_0 is intimately tied with the initial behavior and the final epidemic size (the number of individuals that ever get infected) in SIR models. Loosely speaking, if $R_0 < 1$, then the epidemic will quickly die down and eventually only a tiny fraction of the population will be affected; if $R_0 > 1$, then the epidemic will take off and a considerable proportion of the population will be affected by the disease.

For the deterministic SIR model in (1), the basic reproductive number can be written

as $R_0 = \beta N/\gamma$, whereas for the stochastic SIR model in (2) and (3), $R_0 = \beta \bar{d}/\gamma$, where \bar{d} is the average number of contacts for individuals in the population at the early stage of the epidemic. In temporal network epidemic processes, however, the basic reproductive number does not necessarily carry a clear meaning, nor does it directly relate to the final size of the epidemic (Holme and Masuda, 2015). For our proposed generative model where the epidemic and network *jointly* evolve, the definition and expression of R_0 become even more complicated. Here, R_0 may be vaguely expressed as

$$\frac{\beta}{\gamma} N \times (\text{density of active } S\text{-}I \text{ links among all possible } S\text{-}I \text{ links at “early stage”}),$$

and yet, since social link changes and infection spreading may occur in distinct time scales (in other words, at distinct speeds), the “early stage” of the epidemic process could correspond to various network structures and thus different numbers of active $S\text{-}I$ links, which, in turn, lead to different estimates of the expected number of secondary infections. Previous works (Tunc et al., 2013; Van Segbroeck et al., 2010), have investigated⁵ two simplified, extreme scenarios where the early stage epidemic behavior can be easily described and R_0 has an explicit expression:

1. **Fast network dynamics:** when the rate of link changes is *significantly faster* than that of the infection (and recovery), it can be assumed that the network process has reached a steady state before the disease starts spreading. Then the basic reproductive number is $R_0^{(F)} = \frac{\beta}{\gamma} N \psi_{SI}$, where $\psi_{SI} = \alpha_{SI}/(\alpha_{SI} + \omega_{SI})$ is the expected “density” of $S\text{-}I$ links at the network steady state.
2. **Slow network dynamics:** when the rate of link changes is *much slower* than that of the infection, it can be assumed that the network structure remains the same (as the initial configuration \mathcal{G}_0) when the epidemic process begins. Thus the basic reproductive number is $R_0^{(S)} = \frac{\beta}{\gamma} N p_0$, where p_0 is the density of \mathcal{G}_0 .

The expression of R_0 is unclear when the network and the epidemic evolve at comparable rates, and the concept “basic reproductive number” may not even be meaningful with an

⁵Those are conducted using deterministic, ODE-based methods, but since the expected behavior is studied, the results can be well translated into the stochastic setting.

adaptive network, since the system can exhibit complex behaviors (Kiss et al., 2017) with features and outcomes that cannot be described by a single quantity like R_0 . One possible direction of future work may be to investigate, under the coupled process of epidemics and adaptive networks, the general concept and formula of R_0 , or other metrics that quantitatively describe the systematic behavior.

SUPPLEMENTARY MATERIAL

Supplementary information: Supplementary proofs and derivations, inference details on open population epidemics, and more results from simulation experiments and real data experiments. (.pdf file: `supplement.pdf`)

Codes and examples: R codes for all simulation experiments, accompanied by example synthetic datasets. (Anonymized repository: <https://anonymous.4open.science/r/2231b6ae-00aa-414c-9d6f-37c69084e5a0/>)

References

- Aiello, A. E., A. M. Simanek, M. C. Eisenberg, A. R. Walsh, B. Davis, E. Volz, C. Cheng, J. J. Rainey, A. Uzicanin, H. Gao, et al. (2016). Design and methods of a social network isolation study for reducing respiratory infection transmission: The eX-FLU cluster randomized trial. *Epidemics* 15, 38–55.
- Anderson, R. M. and R. M. May (1992). *Infectious diseases of humans: dynamics and control*. Oxford university press.
- Andrieu, C., A. Doucet, and R. Holenstein (2010). Particle Markov chain Monte Carlo methods. *Journal of the Royal Statistical Society: Series B (Statistical Methodology)* 72(3), 269–342.
- Auranen, K., E. Arjas, T. Leino, and A. K. Takala (2000). Transmission of pneumococcal carriage in families: a latent Markov process model for binary longitudinal data. *Journal of the American Statistical Association* 95(452), 1044–1053.

- Bailey, N. T. et al. (1975). *The mathematical theory of infectious diseases and its applications*. Number 2nd edition. Charles Griffin & Company Ltd 5a Crendon Street, High Wycombe, Bucks HP13 6LE.
- Bansal, S., J. Read, B. Pourbohloul, and L. A. Meyers (2010). The dynamic nature of contact networks in infectious disease epidemiology. *Journal of biological dynamics* 4(5), 478–489.
- Barrat, A., C. Cattuto, A. E. Tozzi, P. Vanhems, and N. Voirin (2014). Measuring contact patterns with wearable sensors: methods, data characteristics and applications to data-driven simulations of infectious diseases. *Clinical Microbiology and Infection* 20(1), 10–16.
- Bell, D., A. Nicoll, K. Fukuda, P. Horby, and A. Monto (2006). World health organization writing group. non-pharmaceutical interventions for pandemic influenza, national and community measures. *Emerg Infect Dis* 12(1), 88–94.
- Britton, T. (2010). Stochastic epidemic models: a survey. *Mathematical biosciences* 225(1), 24–35.
- Cauchemez, S., L. Temime, A.-J. Valleron, E. Varon, G. Thomas, D. Guillemot, and P.-Y. Boëlle (2006). S. pneumoniae transmission according to inclusion in conjugate vaccines: Bayesian analysis of a longitudinal follow-up in schools. *BMC Infectious Diseases* 6(1), 14.
- Clementi, A. E., C. Macci, A. Monti, F. Pasquale, and R. Silvestri (2010). Flooding time of edge-Markovian evolving graphs. *SIAM journal on discrete mathematics* 24(4), 1694–1712.
- Eames, K., N. Tilton, P. White, E. Adams, and W. Edmunds (2010). The impact of illness and the impact of school closure on social contact patterns. *Health technology assessment (Winchester, England)* 14(34), 267–312.
- Edmunds, W., G. Kafatos, J. Wallinga, and J. Mossong (2006). Mixing patterns and the spread of close-contact infectious diseases. *Emerging themes in epidemiology* 3(1), 10.

- Edmunds, W. J., C. O’callaghan, and D. Nokes (1997). Who mixes with whom? a method to determine the contact patterns of adults that may lead to the spread of airborne infections. *Proceedings of the Royal Society of London. Series B: Biological Sciences* 264(1384), 949–957.
- Enright, J. and R. Kao (2018). Epidemics on dynamic networks. *Epidemics*.
- Fintzi, J., X. Cui, J. Wakefield, and V. N. Minin (2017). Efficient data augmentation for fitting stochastic epidemic models to prevalence data. *Journal of Computational and Graphical Statistics* 26(4), 918–929.
- Funk, S., M. Salathé, and V. A. Jansen (2010). Modelling the influence of human behaviour on the spread of infectious diseases: a review. *Journal of the Royal Society Interface* 7(50), 1247–1256.
- Geweke, J. et al. (1991). *Evaluating the accuracy of sampling-based approaches to the calculation of posterior moments*, Volume 196. Federal Reserve Bank of Minneapolis, Research Department Minneapolis, MN.
- Gillespie, D. T. (1976). A general method for numerically simulating the stochastic time evolution of coupled chemical reactions. *Journal of computational physics* 22(4), 403–434.
- Group, W. H. O. W. (2006). Nonpharmaceutical interventions for pandemic influenza, national and community measures. *Emerging infectious diseases* 12(1), 88.
- Hethcote, H. W. (2000). The mathematics of infectious diseases. *SIAM review* 42(4), 599–653.
- Ho, L. S. T., J. Xu, F. W. Crawford, V. N. Minin, and M. A. Suchard (2018). Birth/birth-death processes and their computable transition probabilities with biological applications. *Journal of Mathematical Biology* 76(4), 911–944.
- Hobolth, A. and E. A. Stone (2009). Simulation from endpoint-conditioned, continuous-time Markov chains on a finite state space, with applications to molecular evolution. *The Annals of Applied Statistics* 3(3), 1204.

- Höhle, M. and E. Jørgensen (2002). *Estimating parameters for stochastic epidemics*. [The Royal Veterinary and Agricultural University], Dina.
- Holme, P. and N. Masuda (2015). The basic reproduction number as a predictor for epidemic outbreaks in temporal networks. *PloS one* 10(3), e0120567.
- Hoti, F., P. Erästö, T. Leino, and K. Auranen (2009). Outbreaks of streptococcus pneumoniae carriage in day care cohorts in finland—implications for elimination of transmission. *BMC infectious diseases* 9(1), 102.
- Kermack, W. O. and A. G. McKendrick (1927). A contribution to the mathematical theory of epidemics. *Proceedings of the royal society of london. Series A, Containing papers of a mathematical and physical character* 115(772), 700–721.
- Kiss, I. Z., L. Berthouze, J. C. Miller, and P. L. Simon (2017). *Mapping Out Emerging Network Structures in Dynamic Network Models Coupled with Epidemics*, pp. 267–289. Singapore: Springer Singapore.
- Kiss, I. Z., L. Berthouze, T. J. Taylor, and P. L. Simon (2012). Modelling approaches for simple dynamic networks and applications to disease transmission models. *Proceedings of the Royal Society A: Mathematical, Physical and Engineering Sciences* 468(2141), 1332–1355.
- Kiti, M. C., M. Tizzoni, T. M. Kinyanjui, D. C. Koech, P. K. Munywoki, M. Meriac, L. Cappa, A. Panisson, A. Barrat, C. Cattuto, et al. (2016). Quantifying social contacts in a household setting of rural kenya using wearable proximity sensors. *EPJ Data Science* 5(1), 21.
- Masuda, N. and P. Holme (2013). Predicting and controlling infectious disease epidemics using temporal networks. *F1000prime reports* 5.
- Masuda, N. and P. Holme (2017). *Temporal network epidemiology*. Springer.
- Melegaro, A., M. Jit, N. Gay, E. Zagheni, and W. J. Edmunds (2011). What types of contacts are important for the spread of infections? using contact survey data to explore european mixing patterns. *Epidemics* 3(3-4), 143–151.

- Mossong, J., N. Hens, M. Jit, P. Beutels, K. Auranen, R. Mikolajczyk, M. Massari, S. Salmaso, G. S. Tomba, J. Wallinga, et al. (2008). Social contacts and mixing patterns relevant to the spread of infectious diseases. *PLoS medicine* 5(3), e74.
- Neal, P. J. and G. O. Roberts (2004). Statistical inference and model selection for the 1861 Hagelloch measles epidemic. *Biostatistics* 5(2), 249–261.
- Ogura, M. and V. M. Preciado (2016). Stability of spreading processes over time-varying large-scale networks. *IEEE Transactions on Network Science and Engineering* 3(1), 44–57.
- Ogura, M. and V. M. Preciado (2017). Optimal containment of epidemics in temporal and adaptive networks. In *Temporal Network Epidemiology*, pp. 241–266. Springer.
- O’Neill, P. D. (2009). Bayesian inference for stochastic multitype epidemics in structured populations using sample data. *Biostatistics* 10(4), 779–791.
- Ozella, L., F. Gesualdo, M. Tizzoni, C. Rizzo, E. Pandolfi, I. Campagna, A. E. Tozzi, and C. Cattuto (2018). Close encounters between infants and household members measured through wearable proximity sensors. *PloS one* 13(6), e0198733.
- Pastor-Satorras, R., C. Castellano, P. Van Mieghem, and A. Vespignani (2015). Epidemic processes in complex networks. *Reviews of modern physics* 87(3), 925.
- Pooley, C., S. Bishop, and G. Marion (2015). Using model-based proposals for fast parameter inference on discrete state space, continuous-time Markov processes. *Journal of The Royal Society Interface* 12(107), 20150225.
- Tsang, T. K., V. J. Fang, D. K. M. Ip, R. A. P. M. Perera, H. C. So, G. M. Leung, J. S. M. Peiris, B. J. Cowling, and S. Cauchemez (2019). Indirect protection from vaccinating children against influenza in households. *Nature Communications* 10(1), 106.
- Tunc, I., M. S. Shkarayev, and L. B. Shaw (2013). Epidemics in adaptive social networks with temporary link deactivation. *Journal of statistical physics* 151(1-2), 355–366.

- Van Kerckhove, K., N. Hens, W. J. Edmunds, and K. T. Eames (2013). The impact of illness on social networks: implications for transmission and control of influenza. *American journal of epidemiology* 178(11), 1655–1662.
- Van Segbroeck, S., F. C. Santos, and J. M. Pacheco (2010). Adaptive contact networks change effective disease infectiousness and dynamics. *PLoS computational biology* 6(8), e1000895.
- Vanhems, P., A. Barrat, C. Cattuto, J.-F. Pinton, N. Khanafer, C. Régis, B.-a. Kim, B. Comte, and N. Voirin (2013). Estimating potential infection transmission routes in hospital wards using wearable proximity sensors. *PloS one* 8(9), e73970.
- Voirin, N., C. Payet, A. Barrat, C. Cattuto, N. Khanafer, C. Régis, B.-a. Kim, B. Comte, J.-S. Casalegno, B. Lina, and P. Vanhems (2015). Combining high-resolution contact data with virological data to investigate influenza transmission in a tertiary care hospital. *Infection Control & Hospital Epidemiology* 36, 254.
- Wallinga, J., W. J. Edmunds, and M. Kretzschmar (1999). Perspective: human contact patterns and the spread of airborne infectious diseases. *TRENDS in Microbiology* 7(9), 372–377.

SUPPLEMENTARY INFORMATION

S1 Complete Data Likelihood for SIS-type Contagions

For an SIS-type infectious disease, the complete data likelihood can be derived following the same steps in Section 3.2. Alternatively, one can slightly modify (14) to arrive at the complete likelihood for an SIS-type contagion. Since an individual doesn't acquire immunity upon recovery, it is equivalent to setting $H(t) \equiv S(t)$ at any time t . Thus the complete data likelihood is

$$\begin{aligned} \mathcal{L}(\beta, \gamma, \tilde{\alpha}, \tilde{\omega} | \mathcal{G}_0) \\ = \gamma^{n_R} \beta^{n_E-1} \alpha_{SS}^{C_{SS}} \alpha_{SI}^{C_{SI}} \alpha_{II}^{C_{II}} \omega_{SS}^{D_{SS}} \omega_{SI}^{D_{SI}} \omega_{II}^{D_{II}} \prod_{j=2}^n \left[\tilde{M}(t_j) (I_{p_{j1}}(t_j))^{F_j} \right] \\ \times \exp \left(- \int_0^{T_{\max}} [\beta SI(t) + \gamma I(t) + \tilde{\alpha}^T \mathbf{M}_{\max}(t) + (\tilde{\omega} - \tilde{\alpha})^T \mathbf{M}(t)] dt \right). \end{aligned} \quad (20)$$

S2 Auxiliary Proofs and Derivations

Proof for Theorem 3.1 From (14), we can obtain the log-likelihood:

$$\begin{aligned} \ell(\beta, \gamma, \tilde{\alpha}, \tilde{\omega} | \mathcal{G}_0) &= \log \mathcal{L}(\beta, \gamma, \tilde{\alpha}, \tilde{\omega} | \mathcal{G}_0) \\ &= \sum_{j=2}^n \left[\log \tilde{M}(t_j) + F_j \log (I_{p_{j1}}(t_j)) \right] + n_R \log \gamma + (n_E - 1) \log \beta \\ &\quad + C_{HH} \log \alpha_{SS} + C_{HI} \log \alpha_{SI} + C_{II} \log \alpha_{II} + D_{HH} \log \omega_{SS} + D_{HI} \log \omega_{SI} + D_{II} \log \omega_{II} \\ &\quad - \sum_{j=1}^n [\beta SI(t_j) + \gamma I(t_j) + \tilde{\alpha}^T (\mathbf{M}_{\max}(t_j) - \mathbf{M}(t_j)) + \tilde{\omega}^T \mathbf{M}(t_j)] (t_j - t_{j-1}). \end{aligned} \quad (21)$$

Taking partial derivatives of the right hand side of (21) with respect to the parameters and setting them to zero yield the results above.

S3 Relaxing the Closed Population Assumption

Suppose the observed population is not fully closed, but is a subset of a larger yet unobserved population. Then it is possible for an individual to get infected by an outsider. Let ξ be

the “external infection” rate, the rate for any susceptible individual to be infected by any external infectious source, then the complete data likelihood is

$$\begin{aligned}\mathcal{L}(\beta, \xi, \gamma, \tilde{\alpha}, \tilde{\omega} | \mathcal{G}_0) &= p(\text{epidemic events, network events} | \beta, \xi, \gamma, \alpha, \omega, \mathcal{G}_0) \\ &= \gamma^{n_R} \alpha_{SS}^{C_{HH}} \alpha_{SI}^{C_{HI}} \alpha_{II}^{C_{II}} \omega_{SS}^{D_{HH}} \omega_{SI}^{D_{HI}} \omega_{II}^{D_{II}} \prod_{j=2}^n \left[\tilde{M}(t_j) (\beta I_{p_{j1}}(t_j) + \xi)^{F_j} \right] \\ &\quad \times \exp \left(- \int_0^{T_{\max}} [\beta SI(t) + \xi S(t) + \gamma I(t) + \tilde{\alpha}^T \mathbf{M}_{\max}(t) + (\tilde{\omega} - \tilde{\alpha})^T \mathbf{M}(t)] dt \right). \quad (22)\end{aligned}$$

MLEs for $\{\gamma, \tilde{\alpha}, \tilde{\omega}\}$ remain unchanged, but estimating β and ξ is less straightforward. Let $\ell(\beta, \xi, \gamma, \tilde{\alpha}, \tilde{\omega} | \mathcal{G}_0)$ be the log-likelihood, then the partial derivatives of the log-likelihood w.r.t. β and ξ are

$$\begin{aligned}\frac{\partial \ell}{\partial \beta} &= \sum_{j=2}^n \frac{F_j I_{p_{j1}}(t_j)}{\beta I_{p_{j1}}(t_j) + \xi} - \sum_{j=1}^n SI(t_j)(t_j - t_{j-1}), \\ \frac{\partial \ell}{\partial \xi} &= \sum_{j=2}^n \frac{F_j}{\beta I_{p_{j1}}(t_j) + \xi} - \sum_{j=1}^n S(t_j)(t_j - t_{j-1}),\end{aligned}$$

which do not directly lead to closed-form solutions.

Reparameterizing by $\xi = \kappa\beta$ leads to the following partially derivatives

$$\frac{\partial \ell}{\partial \beta} = \frac{n_E - 1}{\beta} - \sum_{j=1}^n [SI(t_j) + \kappa S(t_j)](t_j - t_{j-1}), \quad (23)$$

$$\frac{\partial \ell}{\partial \kappa} = \sum_{j=2}^n \frac{F_j}{I_{p_{j1}}(t_j) + \kappa} - \beta \sum_{j=1}^n S(t_j)(t_j - t_{j-1}), \quad (24)$$

which are slightly more straightforward in form, and can be solved numerically to obtain the MLEs.

If, somehow, we have information on which infection cases are caused by internal sources and which are caused by external sources, then we can directly obtain the MLEs and Bayesian posterior distributions for all the parameters. For an infection event e_j (with $F_j = 1$), let $\text{Int}_j = 1$ if it is “internal” and let $\text{Int}_j = 0$ otherwise. Then the complete data likelihood can be re-written as

$$\begin{aligned}\mathcal{L}(\beta, \xi, \gamma, \tilde{\alpha}, \tilde{\omega} | \mathcal{G}_0) &= \beta^{(n_E^{\text{int}} - \text{Int}_1)} \xi^{(n_E^{\text{ext}} - 1 + \text{Int}_1)} \gamma^{n_R} \alpha_{SS}^{C_{HH}} \alpha_{SI}^{C_{HI}} \alpha_{II}^{C_{II}} \omega_{SS}^{D_{HH}} \omega_{SI}^{D_{HI}} \omega_{II}^{D_{II}} \prod_{j=2}^n \left[\tilde{M}(t_j) I_{p_{j1}}(t_j)^{F_j \text{Int}_j} \right]\end{aligned}$$

$$\times \exp \left(- \int_0^{T_{\max}} [\beta SI(t) + \xi S(t) + \gamma I(t) + \tilde{\alpha}^T \mathbf{M}_{\max}(t) + (\tilde{\omega} - \tilde{\alpha})^T \mathbf{M}(t)] dt \right), \quad (25)$$

where n_E^{int} and n_E^{ext} are the total numbers of internal and external infection events, respectively.

Estimation for all parameters remains unchanged except for β and ξ . Their MLEs are

$$\hat{\beta} = \frac{n_E^{\text{int}} - \text{Int}_1}{\sum_{j=1}^n SI(t_j)(t_j - t_{j-1})}, \quad \hat{\xi} = \frac{n_E^{\text{ext}} - 1 + \text{Int}_1}{\sum_{j=1}^n S(t_j)(t_j - t_{j-1})}, \quad (26)$$

and with Gamma priors $\beta \sim Ga(a_\beta, b_\beta)$ and $\xi \sim Ga(a_\xi, b_\xi)$, their posterior distributions are

$$\beta | \{e_j\} \sim Ga \left(a_\beta + (n_E^{\text{int}} - \text{Int}_1), b_\beta + \sum_{j=1}^n SI(t_j)(t_j - t_{j-1}) \right), \quad (27)$$

$$\xi | \{e_j\} \sim Ga \left(a_\xi + (n_E^{\text{ext}} - 1 + \text{Int}_1), b_\xi + \sum_{j=1}^n S(t_j)(t_j - t_{j-1}) \right). \quad (28)$$

When there is missingness in recovery times, the Bayesian inference procedure described in Section 4 can still be carried out, with two slight modifications. First, in the data augmentation step, when drawing missing recovery times in an interval $(u, v]$, the DARCI algorithm (Prop. 4.2) inspects \mathcal{I}_p only for each $p \in \mathcal{P}^{\text{int}}$, where \mathcal{P}^{int} is the group of individuals who get *internally* infected during $(u, v]$. Second, in each iteration, parameter values are drawn from the posterior distributions specified in (15) except for β and ξ , for which the posteriors are stated in (27) and (28), respectively.

S4 More Results on Simulation Experiments

Supplement for “inference from complete event data” Figure S1 and S2 complement Figure 2 and 3 in the main text, showing inference results for all the parameters in the corresponding experiments.

Experiments on larger networks Figure S3 shows MLEs and 95% confidence bands for parameters with complete data generated on a network with $N = 500$ individuals. Other experimental settings are the same as those in Section 5.1. With a larger population, there tends to be more events available for inference, so the accuracy is in fact improved.

Experiments on different initial network configurations Still set population size $N = 100$, but instead of a random Erdős–Rényi graph as \mathcal{G}_0 , the initial network is a “hubnet”: one individual (the “hub”) is connected to everyone else in the population while the others form an $ER(N - 1, p)$ random graph, with edge probability $p = 0.1$. Figure S4 summarizes results of Bayesian inference carried out on complete event data generated in this setting.

Supplement for “Assessing model flexibility” Estimate parameters Θ of the full model on datasets generated from 1) the decoupled temporal network epidemic process with type-independent edge rates, and 2) the static network epidemic process where the network remains unchanged. For both simpler models, fix $\beta = 0.03$ and $\gamma = 0.12$, and for the former model, let link activation rate $\alpha = 0.005$ and termination rate $\omega = 0.05$. Still, set population size $N = 100$ and let the initial network be a random Erdős–Rényi graph with edge probability $p = 0.1$.

We present, in Figure S5, the results of Bayesian inference on datasets generated from the decoupled process model. Across four different realizations, it can be observed that, the posterior samples of link activation rates $(\alpha_{SS}, \alpha_{SI}, \alpha_{II})$ concentrate around the same mean, and uncertainty is reduced with more events available for inference. Same can be said about the link termination rates, $\omega_{SS}, \omega_{SI}, \omega_{II}$. This verifies that the proposed model is indeed a generalization of the aforementioned two simpler processes, and the inference method is able to recover the truth under mild model misspecification.

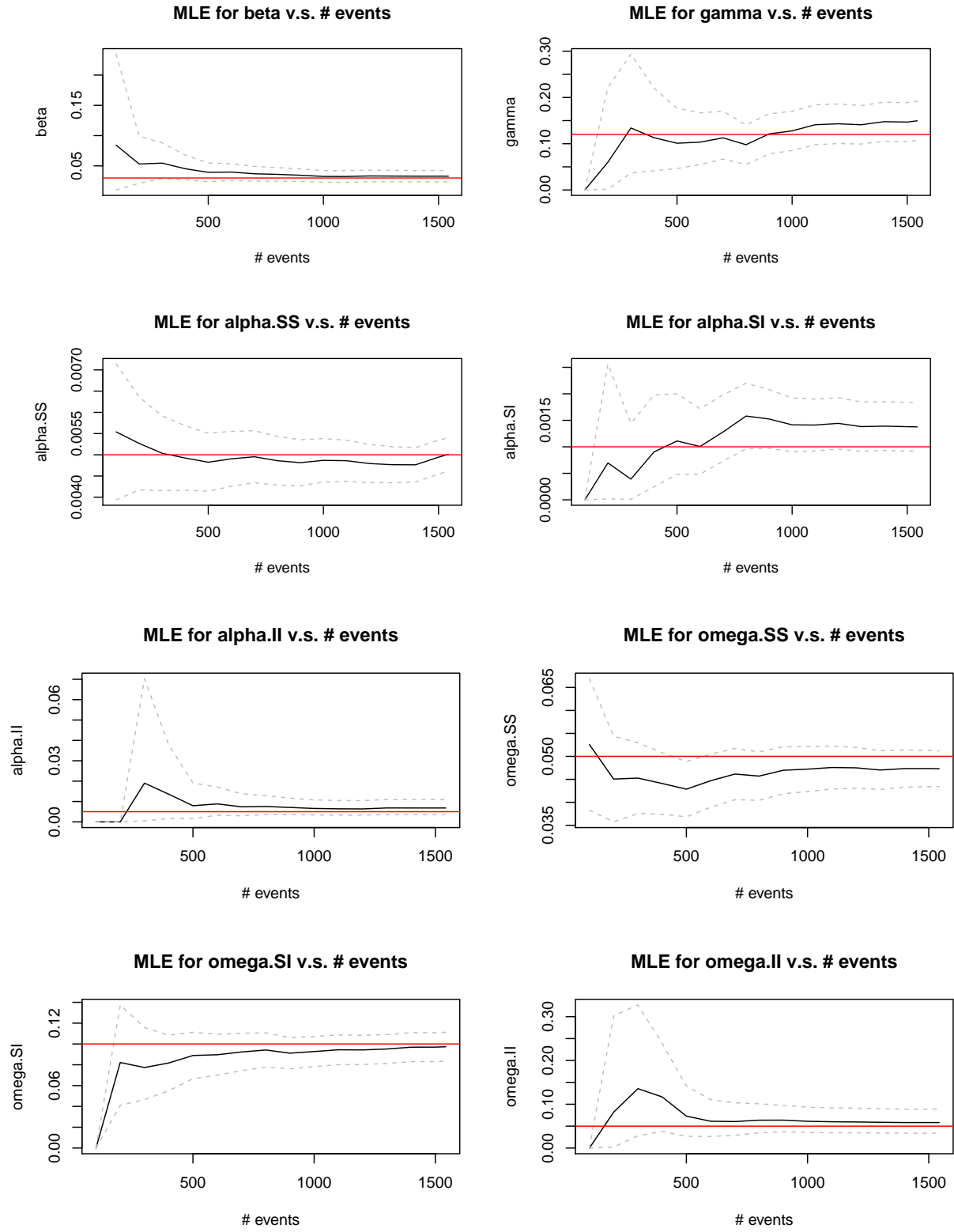


Figure S1: MLEs versus number of events used for inference. Dashed gray lines show the lower and upper bounds for 95% frequentist confidence intervals, and red lines mark the true parameter values.

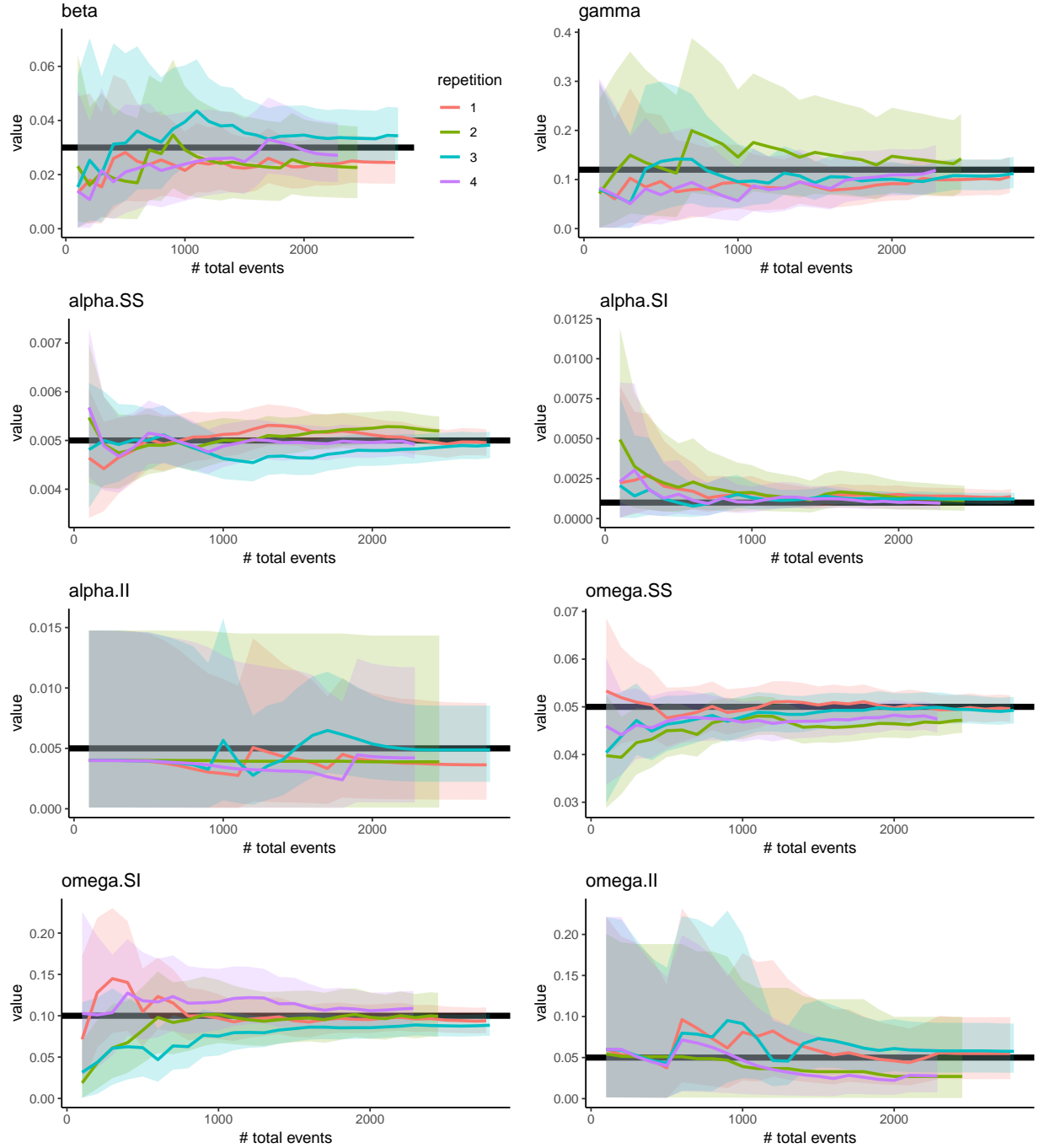


Figure S2: Posterior sample means v.s. number of total events used for inference. True parameter values are marked by **bold dark** horizontal lines, along with 95% credible bands. Results are presented for 4 different complete datasets.

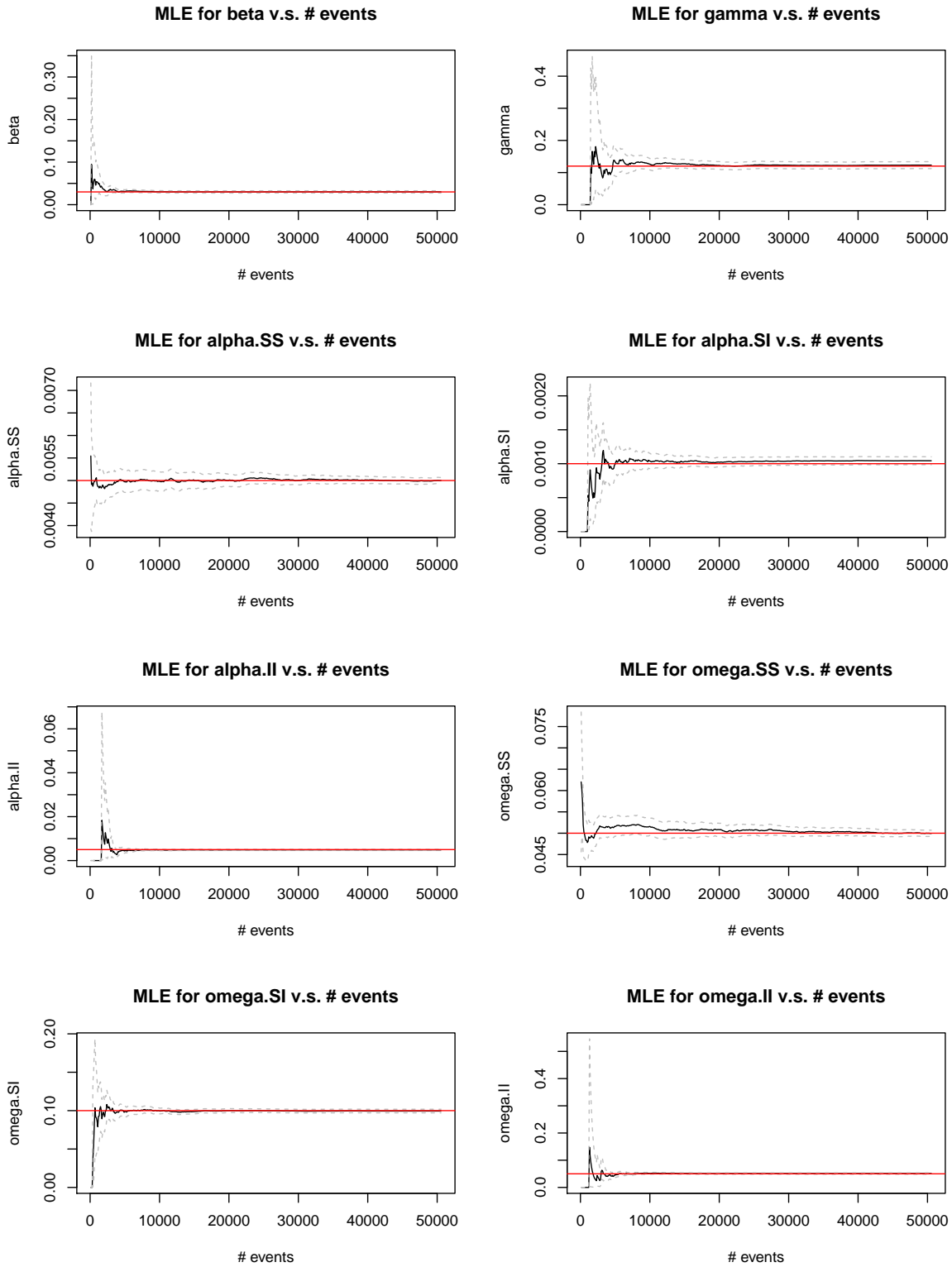


Figure S3: MLEs versus number of total events, on a larger population with $N = 500$. Dashed gray lines show the lower and upper bounds for 95% confidence intervals, and red lines mark the true parameter values. With a larger population size, there tends to be more events, which in fact facilitates estimation.

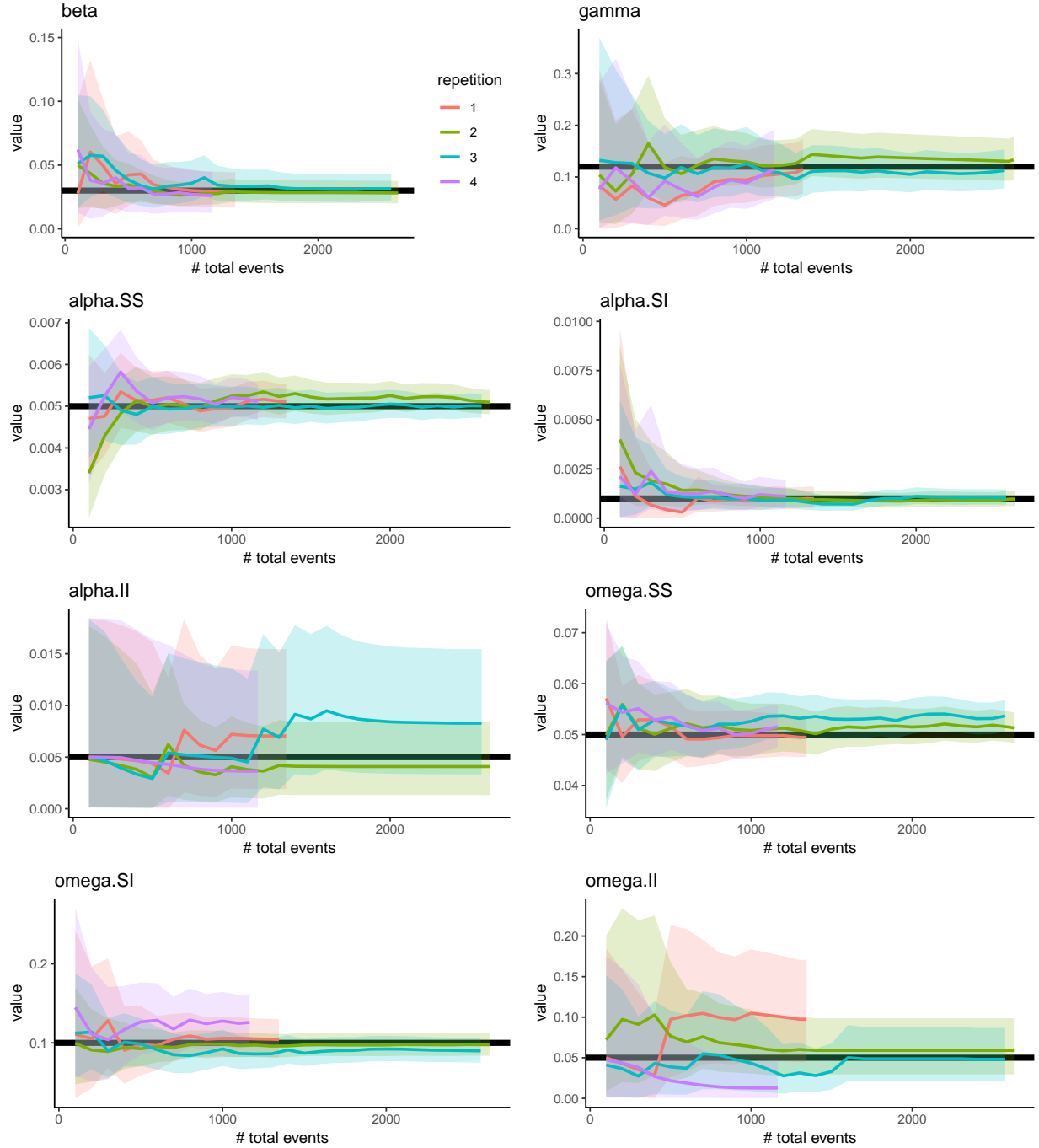


Figure S4: Posterior sample means v.s. number of total events, with \mathcal{G}_0 as a $N = 100$ -node “hubnet”. True parameter values are marked by **bold dark** horizontal lines, along with 95% credible bands. Results are presented for 4 different complete datasets.

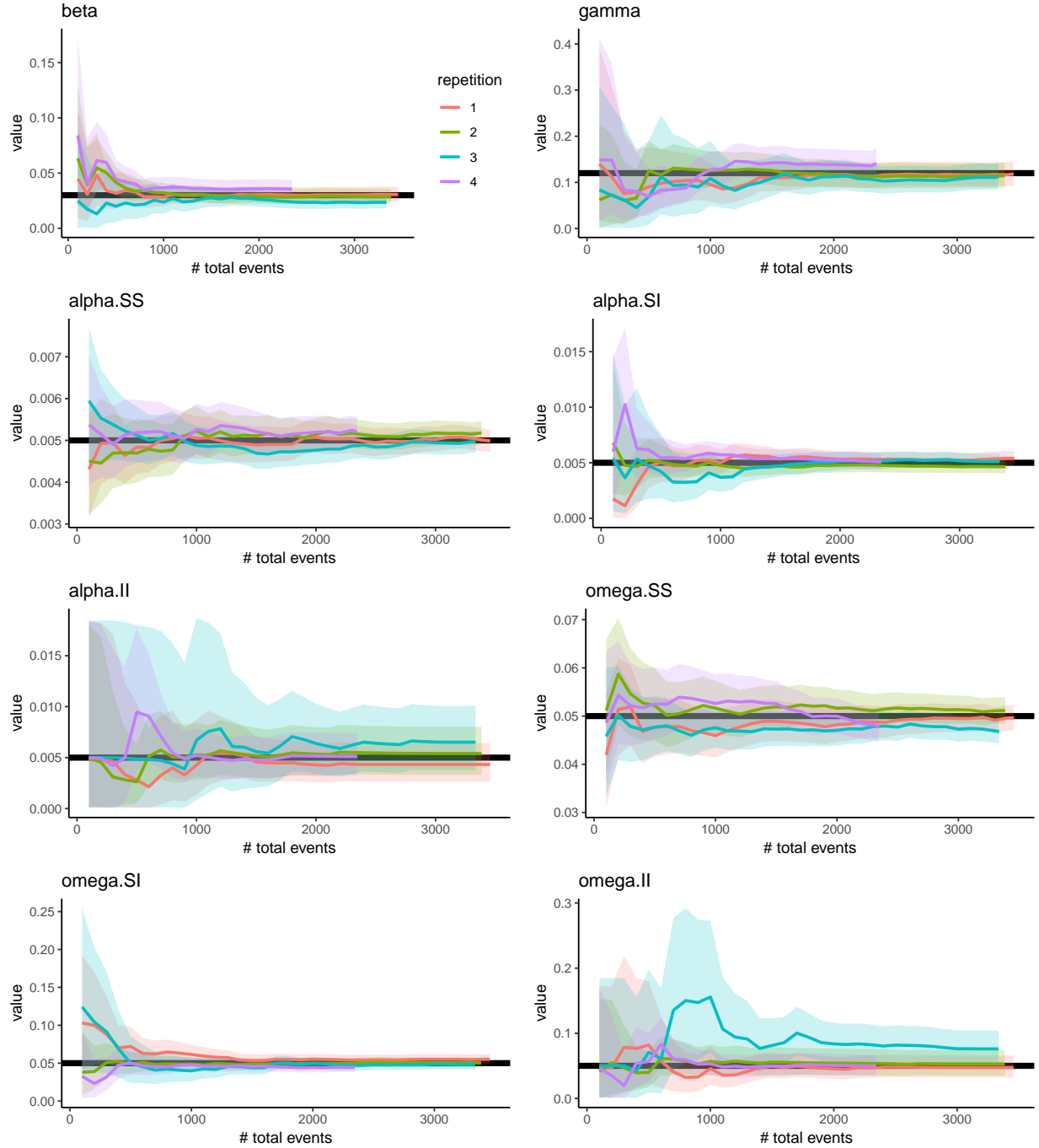


Figure S5: Posterior sample means versus number of total events, estimated using datasets generated by the decoupled process model. True parameter values are marked by **bold dark** horizontal lines, along with 95% credible bands. Results are presented for 4 different complete datasets.

S5 Real Data Experiments

S5.1 Data Pre-processing

All infection events and weekly health statuses of all $N = 103$ individuals are extracted from the weekly surveys. In every survey, study participants were asked if they ever felt ill at all in the past week, if they ever experienced certain symptoms, and, if there were symptoms, when the approximate illness onset time was. We take an “infection” as a positive ILI (influenza-like illness) case, which, following the protocol in Aiello et al. (2016), is defined as a cough plus at least one of the following symptoms: fever or feverishness, chills, or body aches. We further examine each ILI case and only accept one as a positive infection if the individual also indicated that they “felt ill” in the past week, thus eliminating a small number of reoccurring ILI cases for the same participants ⁶. Moreover, since an individual may start exhibiting symptoms at most 3 days *after* getting infected and becoming infectious, for each infection event, we set the “real” infection time as the reported onset time minus a random “delay time” uniformly sampled between 0 and 3 days.

Social link activation and termination events are obtained from the iEpi Bluetooth contact records. Each time two study devices were paired, the iEpi application recorded the unique identifiers of the devices, a timestamp, and a received signal strength indicator (RSSI). Since Bluetooth detection can be activated whenever two devices are within a few meters of each other while the two users may not actually be in contact, we only keep those Bluetooth records with relatively strong signals (high values of RSSIs) ⁷. If two consecutive Bluetooth records for one pair of devices are no more than 7.5 minutes apart in time ⁸, then the two records are considered to belong to one single continuous contact; a social link between two individuals is activated at the time of the first Bluetooth detection record in a series of consecutive records that belong to a single contact, and the link is terminated at a random

⁶One particular individual had positive ILI cases and felt ill in week 2, 3, and 5, but not in week 4. We therefore treat his/her illness as an extended one, starting in week 2 and lasting till week 5.

⁷The RSSIs range from -109 to 6, and we set the threshold as -90, so only those records with RSSIs larger than -90 are kept.

⁸We choose 7.5 minutes as a threshold instead of 5 minutes to accommodate potential lapses in Bluetooth detection.

time point between 1 and 6 minutes after the last Bluetooth detection of a continuous contact.

The resulting processed data contain 24 infection events in total, with 14 before the spring break week and 10 after, as well as 45,760 social link activation and termination events. The weekly disease status (healthy or ill) of every participant can be acquired from the weekly surveys, so we know, for example, if an individual recovered sometime after day 7 and before day 14, but the exact times of all recoveries are unknown.

S5.2 Maximum Likelihood Estimation

Instead of assuming the knowledge of which infection cases are internal and which are external, we directly estimate all the parameters based on the likelihood function in (22), solving (23) and (24) for the MLEs of β and ξ .

However, the real data are incomplete, with the exact times of all the recoveries unobserved. We resolve this issue using a naive imputation method—for each recovery, an event time is randomly sampled from a uniform distribution between the time of infection and the earliest time point the individual no longer felt ill (in response to the weekly surveys). Such imputation, of course, is subject to a considerable level of uncertainty, so we randomly generate 10 differently imputed datasets, obtain the MLEs from every dataset, and then report the averages over the 10 runs (see Table S1).

We can see that the MLEs acquired in this manner generally agree with the Bayesian estimates in Section 6.2.

Table S1: MLEs for model parameters using imputed data with all recovery times randomly sampled. The table presents average estimates as well as the standard deviations of estimates over 10 different, randomly imputed datasets. Results generally agree with those acquired using the proposed Bayesian data augmentation inference method.

Parameter	Avg. estimate	Std. deviation
β (internal infection)	0.0676	0.0092
ξ (external infection)	0.00320	1.11×10^{-6}
γ (recovery)	0.236	0.012
α_{SS} (S - S link activation)	0.0530	0.0001
ω_{SS} (S - S link termination)	42.15	0.105
α_{SI} (S - I link activation)	0.0704	0.0028
ω_{SI} (S - I link termination)	52.21	3.83